COMPUTER AIDED EVALUATION OF GEAR TOOTH STRESSES BY FINITE ELEMENT METHOD

A MASTER'S THESIS

Mechanical Engineering
University of Gaziantep

By
Ömer EYERCİOĞLU

August 1990

Approval of the Graduate School of Natural and Applied Sciences

Prof. Dr. Mazhar UNSAL
Director

I certify that this thesis satisfies all the requirements as a thesis for the degree of Master of Science in Mechanical Engineering Department.

Assoc. Prof. Dr. Sedat BAYSEC
Chairmen of the Department

We certify that we have read this thesis and in our opinion it is full adequate, in scope and quality, as a thesis for the degree of Master Science in Mechanical Engineering Department.

Assoc. Prof. Dr. I.Huseyin FILIZ
Supervisor

Examining Committee in Charge

Assoc. Prof. Dr. Servet BUYURAN

Assoc. Prof. Dr. Sedat BAYSEC

Assoc. Prof. Dr. I.Huseyin FILIZ

Assoc. Prof. Dr. Celal KORASLI

Assist. Prof. Dr. A.Ihsan SONMEZ

ABSTRACT

COMPUTER AIDED EVALUATION
OF SPUR GEAR TOOTH STRESSES
BY FINITE ELEMENT METHOD

EYERCIOGLU, Omer
M.S. in Mechanical Engineering
Supervisor : Assoc. Prof. Dr. I. Huseyin FILIZ
August 1990

In this thesis, the spur gear tooth stresses are evaluated by using Finite Element Method. For this purpose a Finite Element Stress Analysis (FESA) package is developed.

The first stage of this study is the modeling of a spur gear and a rack teeth by taking the physical structures of them into account. The spur gear and rack profiles are automatically generated by the program. The value of force and the location of it are dependent on the user's choice. The program gives three option to the user for the determination of forcing point. These are ; tip loading, the highest point of single tooth contact or any other point that is given by user. The location of the highest point of single tooth contact is determined by the program itself. Gauss elimination with back substitution method is used for solving the systems of equations.

With the developed program, several runs are made for different spur gears. The obtained results are compared with previous works. Additionally, the distribution of stresses on the tooth surface and along the weakest section are demonstrated. The effects of gear parameters on stresses are inspected and presented graphically.

Key words : Computer Aided Design, Finite Element, Involute gear, gear tooth stresses.

ÖZET

SONLU ELEMANLAR METODU KULLANILARAK DÜZ DIŞLILERDE DIŞ DIBI GERILMELERININ BILGISAYAR YARDIMI ILE BELIRLENMESI

EYERCIOGLU, Ömer

Yüksek Lisans Tezi : Makina Müh. Bölümü
Tez yöneticisi : Doç. Dr. I. Hüseyin FILIZ
Ağustos 1990

Bu tezde, düz dişlilerde diş dibi gerilmeleri Sonlu Elemanlar Metodu kullanılarak bilgisayar yardımıyla belirlenmiştir.

Bu çalışmada öncelikle düz dişlilerin fiziksel özelliklerine uygun bir model geliştirilmiştir. Bu proğram ile dişli profili bütün özellikleri göz önüne alınarak bilgisayar tarafından oluşturulabilmektedir. Diş üzerine etkiyen kuvvetin değeri ve uygulama noktası kullanıcı tarafından, sunulan şu üç seçenekle belirlenmektedir. Bunlar ; dişin tepe noktası, tek dişin bütün yükü taşıdığı en yüksek nokta veya kullanıcı tarafından tanımlanacak herhangi bir nokta olabilir. Kullanıcının tek dişin bütün yükü taşıması halini seçmesi ile proğram bu noktayı kendiliğinden bulmaktadır. Denklem sisteminin çözümünde Gauss Metodu kullanılmıştır.

Geliştirilen bu Sonlu Elemanlar Analiz paketi değişik dişliler için kullanılarak, diş dibi gerilmeleri bulunmuş ve önceki çalışmalarla

karşılaştırılmıştır. Ayrıca, diş yüzeyi ve dişin en zayıf olduğu çizgi boyunca gerilmelerin dağılımı elde edilmiştir. Dişli parametrelerinin gerilmelere etkileri incelenerek grafiklerle sunulmuştur.

Anahtar kelimeler : Bilgisayar destekli tasarım, Sonlu Elemanlar, evolvent dişli, diş-dibi gerilmeleri.

ACKNOWLEDGEMENT

The author is greatful to Assoc. Prof. Dr. I. Huseyin Filiz for his encouragements and suggestions throughout the study of this thesis as the supervisor.

He also wishes to thank,

Assistants of Mechanical Engineering Department, especially to Mr.M. Cengiz Kayacan for his helps in typing,

Miss. Aysegul Dalbudak for her kindly helps,

Assoc. Prof. Dr. Celal Korasli and persons of computer center for their advice in using the computer facilities.

TABLE OF CONTENTS

LIST OF TABLES

LIST OF FIGURES

Figure Page

NOMENCLATURE

a Addendum

b Dedendum

C The distance between the centers of two mating gears

D Addendum circle diameter of mating gear

ε Contact ratio

ε Strain in *a* direction

F Force acted on gear tooth

f Force vector

g Traveled distance of contact point on the tooth surface

h The height of the point of tangency of fillet radius and gear tooth profile

J AGMA factor

K Stiffness matrix

m Module

N No. of equations in solution matrix

NG No. of teeth on gear

NP No. of teeth on pinion

RA Addendum circle radius

RB Base circle radius

RD Dedendum circle

S The point of tangengy of involute curve and fillet radius

t Tooth thickness in the weakest section

u Nodal displacement in x-direction

U Nodal displacement vector

v Nodal displacement in x-direction

Y Lewis form factor

Z The length of contact

z No. of teeth on teeth

α Angle between the tooth centerline and a point on involute profile

β Force Angle

λ Angle between the tooth centerline and point S

ψ Angle between the points S and Q

θ Angle of radial line of force point with its tangent line to base circ.

ϕ Pressure angle

σ_1, σ_2 Principal stresses

σ_c Maximum compression angle

σ_t Maximum tangential stress

τ_{max} Maximum shear stress

CHAPTER 1

INTRODUCTION

Bending strength of gear tooth is one of the important factors which influence the load carrying capacity of the gears.Many studies have been reported concerning with the stress at the root of gear tooth. The classical approach to the problem of stress determination in gear teeth rests on the cantilever beam theory, with the consideration of *stress concentration factors* which take the radii of curvature in the tooth fillet into account.

Although the semi-empirical equations for stress concentration factors provide valuable information on the stress concentrations of gear teeth, they are still not very widely used in gear design. This is mostly because of the difficulty of the graphical analysis which is required in making a layout of a gear tooth.

During the last decade, the progress of the Finite Element Method (FEM) has made possible the precise estimations of the stress. The development of finite element techniques now permits an exact computation of these stresses. Several private firms and technical institutes already carried out such computations, but their results do not seem to have been throughly published, nor did they have any bearing on the national standards in the field of gear power capacity rating.

The aim of this study is to evaluate the tooth stresses of spur gears and racks by using Finite Element Method. The emphasis is given to involute spur gears with different pressure angles, modules, and contact ratios.

The computer program prepared for this purpose at the first stage starts with the determination of gear tooth geometry and performs mesh generation. After that, according to the number of teeth of the driven and the driver gears, it determines the application of the point of the force at the highest point of single tooth contact. Then stiffness matrix is evaluated and forces at nodal points, deflections and stresses are determined.

The determination of the gear tooth geometry should be in a correct degree of accuracy and yet sufficiently simple to maintain the cost of computation at an acceptable level. Because of the nature of Finite Element Method, the accuracy of the results depends very much on the mesh design of the model. The best results can be drived only through several trials for different structures. In order to ease on the testing of different structures automatic mesh generation is prepared.

To reduce computer storage requirements, an efficient storage structure (column-wise storage order) is chosen, because it is easier to implement than the row-wise order.

The computer program is designed in such a way that anybody who has brief knowledge on FEM can use it easily. Module, addendum, dedendum, pressure angle, number of teeth of driver and driven gears and tooth fillet radius are main input to the program. The value of force transmitted and the decision on where this force is to apply (at the tip of the tooth, the highest point of single tooth contact or any other point) are also given at the start of the execution of the program. All nodal forces, displacements and element stresses are calculated and are output in an organized form.

Simple gear trains with different pressure angles, modules,number of teeth and fillet radius are tested with this program and results are compared with the previous works.

CHAPTER 2

LITERATURE SURVEY

2.1 INTRODUCTION

This chapter gives a brief survey of the most relevant literature related to the study reported in this thesis. In section 2.2 the works on theoretical determination of gear tooth stresses are reviewed. The work on Finite Element Stress Analysis is discussed in section 2.3

2.2 THEORETICAL DETERMINATION OF GEAR TOOTH STRESSES

The strenght of a gear tooth was first calculated to a close degree of accuracy by Willfred LEWIS [1] in 1892. He conceived the idea of inscribing a parabola of uniform strength inside a gear tooth. He observed that when a parabola is made into a cantilever beam, the stress is constant along the surface of the parabola.He considered the shape of gear tooth (form factor) but did not take the stress concentration factor into account.

In the German Standard DIN 3990 [2] a nominal bending stress is used as a basis for computing the tooth strength ; the dependence of the dedendum strength on the size of the fillet radius is represented by a notch-effect factor which is dependent on the material and the surface finish.

In AGMA Standard 220.2 [3] where a similar procedure is followed, a combined nominal bending and compressive stress is used as a basis. The

nominal stress is multiplied by a stress concentration factor which is based on the photoelastic tests carried out by Dolan and Broghamer [4]. This factor takes into account the dependence of the stresses on the size of the fillet and on the location of the loading point.

Niemann [5] uses a nominal stress composed of bending, compresive, and shearing stresses. In that case, the shearing stress contribution is chosen in such a way that for the tooth forms investigated in [6] the stress concentration factor becomes approximately independent of the location of the loading point on the tooth flank. The influence of the fillet radius and the material are represented by a notch-factor.

Heywood [7] represents the tooth through an equivalent trapezoid profile and introduces proximity and stress concentration factor. A similar procedure was proposed by Kelley and Pedersen [8] in continuation of the work by Dolan and Broghamer.

R. G. Mitchiner and H. H. Mabie [9] investigated tooth stresses. They presented a simple and direct approach to the problem of definition of the root profile for standard and non-standard external spur gear teeth. They gave equations and developed a computer program to compute the Lewis form factor Y, and the AGMA geometry factor J. They located the point of interest on the root profile to calculate stresses developed. This work is also reported by Shigley [10].

Yelle [11] developed a set of equations and programmed them in BASIC to calculate the Lewis form factor, by tracing the procedure stated in Ref [12]. He further calculated the tooth deformation, the load transfering points and the load sharing for a large variety of gear pair geometries material combination.

N. K. Al-Id [13], presented a purely theoretical method, based on experimental work of Dolan and Broghamer, in order to determine the stress concentration factors at the tensile fillets of spur gear tooth.

2.3. FINITE ELEMENT STRESS ANALYSIS

Although the label "finite element method " first appeared in 1960, when it was used by Clough [14] in a paper on plane elasticity problems, the ideas of finite element analysis date back much further. In fact, the questions "Who originated the FEM and when did it begin ?" have three different answers depending on the whether one asks an applied mathematician, a physicist, or an engineer. Each of these specialists has some justification for claiming the FEM as his own because each developed the essential ideas independently at different times and for different reasons. The applied mathematicians were concerned with boundary value problems of continuum mechanics; in particular, they wanted to find approximate upper and lower bounds for eigenvalues. The physicists were also interested in solving continuum problems, but they sought means to obtain piecewise approximate functions to represent their continuous functions. Faced with increasingly comlex problems in the aeroelasticity field, the engineers were searching for a way in which to find the stiffness influence coefficients of shell-type structures reinforced by ribs and spars. The efforts of these three groups resulted in three sets of papers with distinctly different viewpoints.

The first efforts to use piecewise continuous functions defined over triangular domains appear in the applied mathematics literature with the work of Courant [15] in 1943. Motivated by Euler's [16] paper, Courant used as an assemblage of triangular elements and the principle of minimum potential energy to study the St. Venant torsion problem. After Courant's work, nearly a decade passed before the discretization ideas were used again. The works of Polya [17,18], Hersch [19], and Weinberger [20,21], who focused their attention on bounding eigenvalues, mark a period of renewed interest.

In 1959, Greenstadt [22], motivated by a discussion in the book by Morse and Feshback [23] outlined a discretization approach involving *cells* instead of points; that is, he imagined the solution domain to be divided into a set of contiguous subdomains. In his theory, he describes a

procedure for representing the unknown function by a series of functions, each associated with one cell.After assigning approximating functions and evaluating the appropriate variational principle in each cell, he uses continuity requirements to tie together the equations for all the cells. By this means, he reduces a continuous problem to a discrete one. Greenstadt's theory allows for irregularly shaped cell meshes and contains many of the essential and fundamental ideas that serve as the mathematical basis for the finite element method as we know it today.

In the early 1960's (about the same time the finite element concepts began to develop in the engineering community), the significant works of White [24] and Friedrichs [25] appeared. These authors, apparently unaware of the engineering activities at that time, used triangularly shaped elements to develop difference equations from variational principles. Although they used regular meshes, they recognized the need for making special provisions at irregular boundaries.

As the popularity of the FEM began to grow in the engineering and physics communities, more applied mathematicians became interested in giving the method a firm mathematical foundation. As a result, a number of studies were aimed at estimating discretization error, rates of convergence, and stability for different types of finite element approximations. These studies most often focused on the special case of linear elliptic boundary value problems. Although the FEM has been and is being frequently applied to non-linear problems [26], corresponding mathematical studies of convergence and accuracy for non-linear problems have seldom appeared.

A fundamental consideration in the FEM (the development of suitable function approximations to field variables) has been advanced by some of the mathematical literature on spline functions [27-35].

Since the late 1960's, the mathematical literature on the FEM has grown more than in any previous period. Several books and monographs [36-39] are devoted to the mathematical foundations of

the method. A survey paper by Oden [40] summarizes for the interested reader some of the recent and sailent mathematical contributions.

Concepts of method began to solidify after 1963 when Besseling [41], Melosh [42], Fraeijs de Veubeke [43], and Jones [44] recognized that the FEM was a form of the Ritz method and confirmed it as a general technique to handle elastic continuum problems. In 1965, the FEM received an even broader interpretation when Zienkiewics and Cheung [45] reported that it is applicable to all field problems which can be cast into variational form. During the late 1960's and early 1970's (while mathematicians were working on establishing errors, bounds, and convergence criteria for the finite element approximations), engineers and other appliers of the FEM were also studying similar concepts for various problems in the area of solid mechanics. Several of these studies [46-56], although restricted to certain types of problems, have yielded useful results.

Because of the large number of equations and corresponding data involved, the finite element analysis is possible only when applied on a computer.So that, the development of FEM is largely depend also on the development of fast computers. The finite element method is readily programmed for high-speed digital computers and in fact the procedure would be little use if computers not available to solve the simultaneous equations that result from the discretization process.

A number of very large capacity finite element programs have been developed. The earlier ones were highly specialized application programs and were often written in machine language. The similarity of program structure which was recognized in the course of different applications led to the development of more sophisticated general systems. The ASKA (developed under Prof. J. H. Argyris at Stuttgart, Germany) program was an early example of such a development; it too was highly machine oriented. In applications for aerospace type problems the capability to solve the problem at all levels is emphasized and efficiency of the system for smaller size analyses is considerably impaired.

The rapid development of successive generations of computers has made it essential to write programs that are easily interchangeable from machine to machine. The availability of fortran as such a language has led to its use for most of the programming effort associated with finite elements.

The NASA (National Aeronautical Space Administration,USA) program represents an attempt to create a flexible programming system for application to the large scale research and development problems of the American aerospace industry.

Application of FEM for the evaluation of gear tooth stresses is seen in early 1970's. In 1974, G. Chabert, T. Dang Tran and R. Mathis [57] have presented a work on stresses on a spur gear tooth and compare the results with ISO and AGMA standards. They expressed their results by the following formulas;

$$\sigma_t=\left[3+\left(38-50\frac{\rho}{m}\right)\left(\frac{1}{z}\right)\right]\frac{F}{mb\varepsilon}$$

$$\sigma_c=\left[3.5+\left(41-50\frac{\rho}{m}\right)\left(\frac{1}{z}\right)\right]\frac{F}{bm\varepsilon}$$

where F is the nominal load acting along the line of action. They have used Henroit's approach which is tha loading force is applied at the tip of the tooth after division by the contact ratio.

The maximum tensile stress at the root of gear tooth and the deflection at the loading point along the line of action were computed by T. Tobe, M. Kato and K. Inoue [58] in 1979. From the computing results, the emprical formula for the maximum tensile stress (kgf/mm^2) due to a normal load P (kgf) was obtained as follows;

$$\sigma_{to} = \frac{P_n}{bm}\left[a_1\left(\frac{1}{z}\right) + a_2\left(\frac{1}{z}\right)^3 + 3.5\right]\exp\left[\left(2.5\left(\frac{1}{z}\right) - 0.5\right)\frac{\lambda}{m}\right]$$

$$a_1 = 2.5 - 18.00\, X_v$$

$$a_2 = 2600 \exp\{-2.75\, X_v\} \qquad (X_v < 0.4)$$

$$a_2 = 2600 \exp\{-2.75 * 0.40\} \qquad (X_v \geq 0.40)$$

where, m: module (mm), b: face width (mm), z: number of gear tooth, X : addendum modification coefficient, λ : distance from the tip.

Drago and Pizzigati [59] have done extensive research of gear stress problem using FEM and have found that FEM is a good approach for investigating the rim effect on tooth fillet stresses. Moreover, it can also be used to establish stress history by subsequently changing tooth contact loading condition for a number of points along the line of action. They showed that their results were about 12 % higher than the calculations reported by AGMA.

Dr. Giovanni Castellani and V. P. Castelli [60] made a considerable study of the proposed ISO strength rating method compared with established AGMA standard methods. They presented comparative geometry factors for strength base on several spur and helical gear designs. The differences in results were so great that it requires more work relating to calculations of stress correction factors.

The work presented by Jeng-Fong Hwang, Dennis A. Guenther and Wiechel J. F. [61] in 1988, provides information about the behaviour of internal spur gears under specific conditions. They have shown that the rim thickness has a dramatic effect on the fillet stresses and stress distribution. They have also found that the root fillet radius has a local effect.

H. von Eiff, K. H. Hirschmann, and G. Lencher [62] studied on the influence of gear tooth geometry on tooth stress of external and

internal gears. For minimizing gear tooth stress, they have studied on many parameters, essentially on the type of cutters. They have shown that the pinion type of cutters with a small number of teeth generate gear tooth fillets which show reduced stress than rack type of cutters.

CHAPTER 3

GEOMETRY AND THEORY OF GEARS

3.1. INTRODUCTION

Tooth geometry and basic theory of spur gears are reviewed in this chapter.

Geometry of spur gear tooth is explained in section 3.2. In section 3.3 and 3.4 load sharing mechanism and the worst loading condition are discussed. Strength of gear teeth is studied in section 3.5.

3.2. GEOMETRY OF SPUR GEAR TOOTH

Spur gears are used to transmit rotary motion between parallel shafts; they are usually cylindrical in shape, and the teeth are straight and parallel to the axis of rotation.

The terminology of spur gear and rack is illustrated in Figure 3.1. A rack is a section of spur gear with an infinitely large pitch diameter. The relation between module and pitch diameter can be written as:

$$M=\frac{D}{N} \qquad (3.1)$$

where M is the module (mm), D is pitch diameter (mm) and N is the number of teeth.

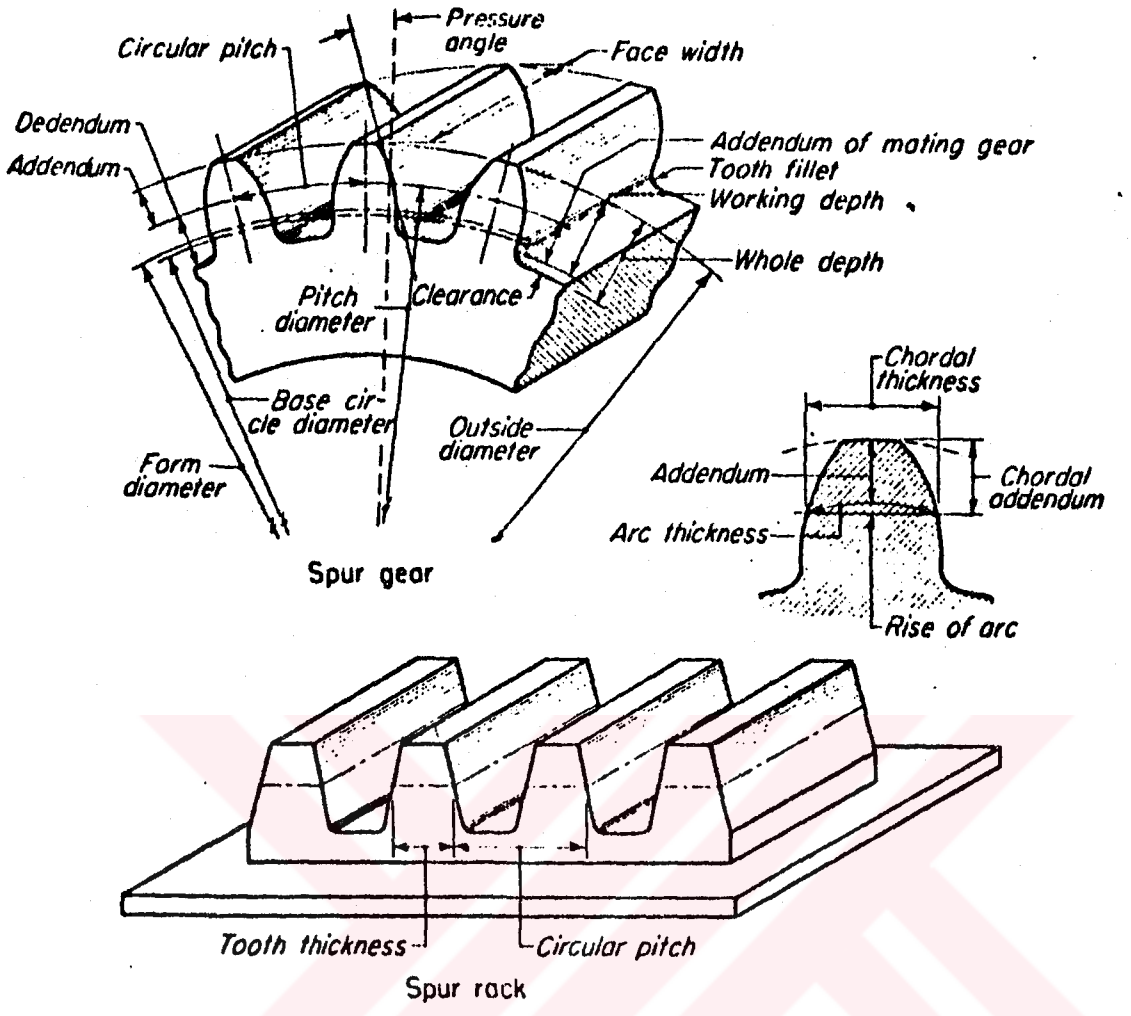

Figure 3.1. Spur-gear and Rack Terminology

The main function of gear tooth profiles is to provide constant angular-velocity ratio during meshing which is known as *conjugate action*. Although there are many types of profiles that will give conjugate action, involute profile which is in universal use, is the only profile which we shall consider in this work.

An involute gear tooth form consists of two similar involute curves with a common base circle as shown in Figure 3.2.

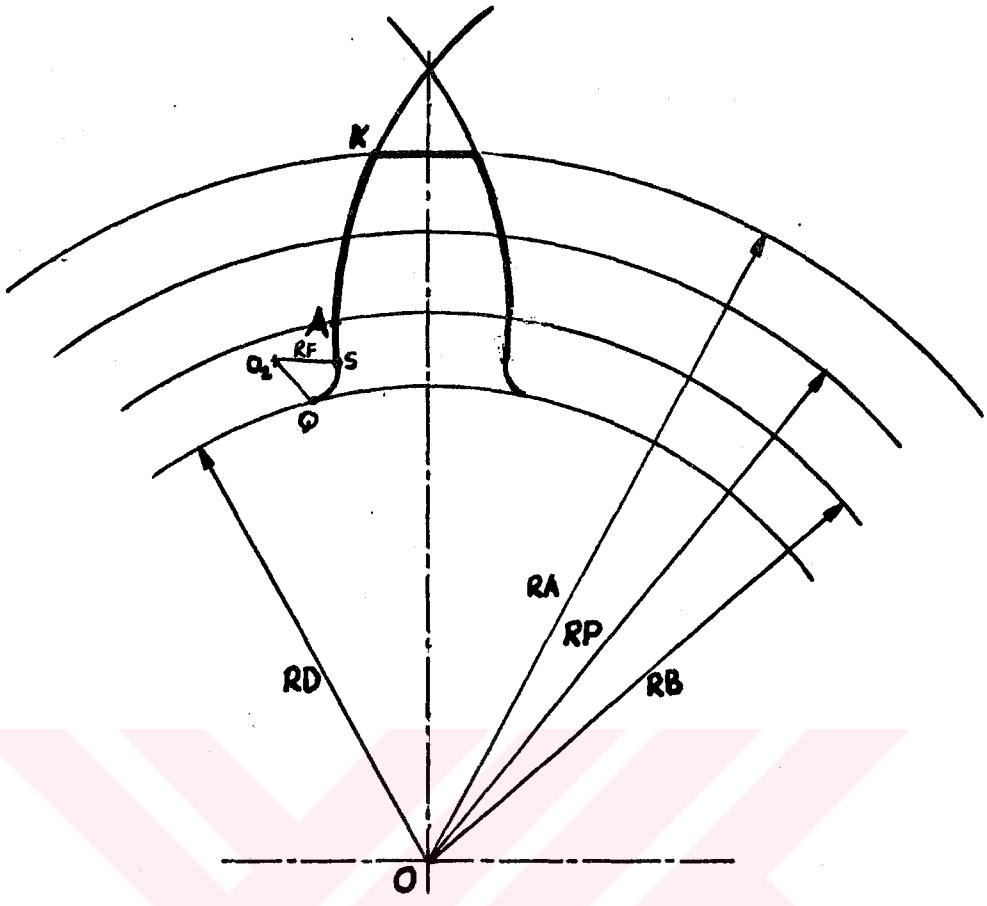

Figure 3.2. Involute Spur Gear Tooth Profile

The starting point of involute curve is on the base circle, that is point A in the figure. Point Q is on the dedendum circle and the point s is on the line tangency of fillet circle to involute curve from point A.

Location of point S is described with the following inequalities;

If (RB-RD) < RF point S is above point A
If (RB-RD) = RF point S is coincident with point A
If (RB-RD) > RF point S is below point A

Since most of the gears are produced in such a way that the difference of base and dedendum radii is greater than fillet radius, it is the third case considered in this study.

Involute profile is generated from point A to K. In general,the involute profile is generated by first determining their relative positions at the base circle, and then adding or subtructing the vectorial angle of the involute for any other radius. This process of calculating involute gear-tooth relationships is called *involumetry.*

Using Figure 3.3, the equation for the involute can be written as;

$$\text{Cos}\,\theta=\frac{RP}{R}\text{Cos}\phi \qquad (3.2)$$

$$\alpha=\frac{\pi}{2N}+(\text{Tan}\phi-\phi)-(\text{Tan}\theta-\theta) \qquad (3.3)$$

The most convenient form for the value of α is in circular measure of radians, and its value can be obtained by subtracting the value of the angles Θ and ϕ expressed in radians from the values of their tangents. The load angle, β, is also required for the evaluation of the gear tooth stress and it is determined as follows ;

$$\beta=\theta-\alpha \qquad (3.4)$$

The above equations are valid only for involute section (from point A to K) on a tooth profile. Below the base circle the tooth profile is not involute. Using Figure 3.3, this non-involute portion can be found by determining the locations of points Q and S.

For the location of Q and S, angles θ and λ must be known. Since point Q is on the dedendum circle and O Q is equal to fillet radius, the angles θ and λ can be expressed as follows ;

$$\lambda=\frac{\pi}{2N}+\text{Tan}\phi-\phi \qquad (3.5)$$

$$\psi=\text{Sin}^{-1}\left(\frac{RF}{RF+RD}\right) \qquad (3.6)$$

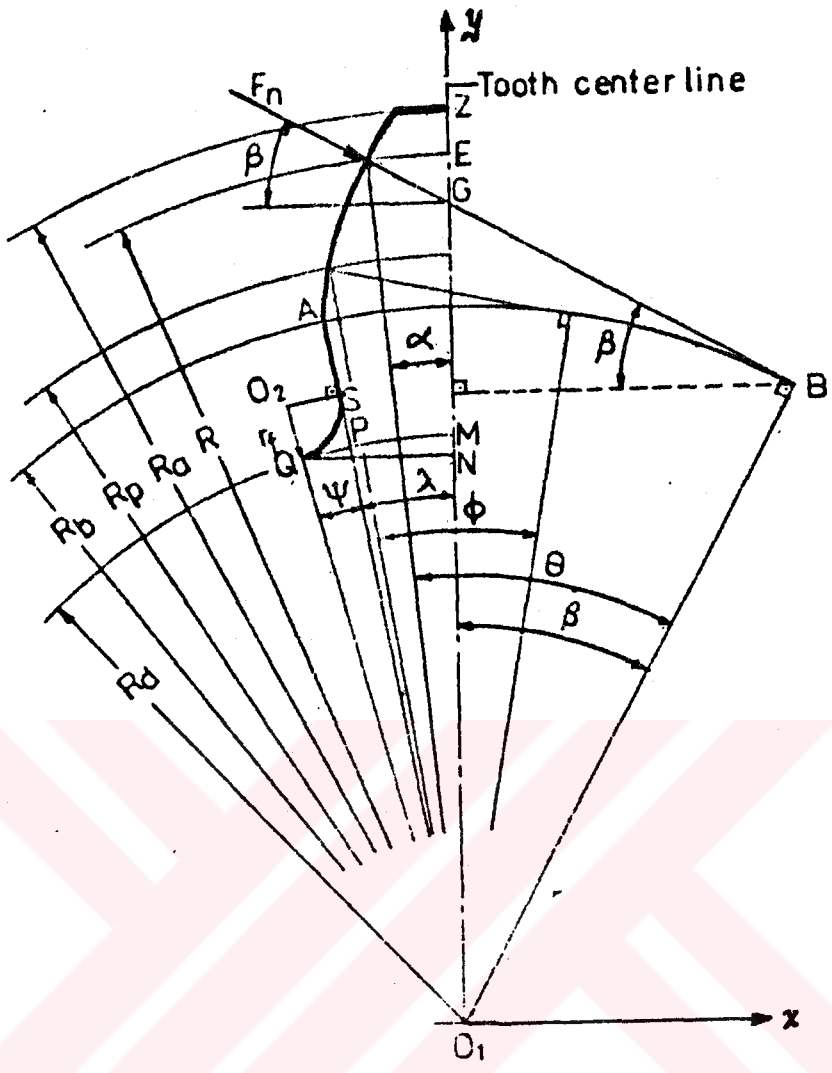

Figure 3.3. Positions of Important Points on a Spur Gear Tooth

The point of tangency S of the fillet circle is at the radial line AO of the tooth profile, and that point A is above S. For this case (RB-RD) > RF.

By using above equations, the positions of Q and S can be found as follows;

$$Q_x = RD\ Cos(\lambda+\psi) \tag{3.7}$$

$$Q_y = RD\ Sin(\lambda+\psi) \tag{3.8}$$

$$O_{2x} = (RD+RF)\ Cos(\lambda+\psi)$$

$$O_{2y}=(RD+RF)\,Sin(\lambda+\psi)$$

$$S_y=O_{2y}+RF\,Sin\lambda \qquad (3.9)$$

$$S_x=O_{2x}-RF\,Cos\lambda \qquad (3.10)$$

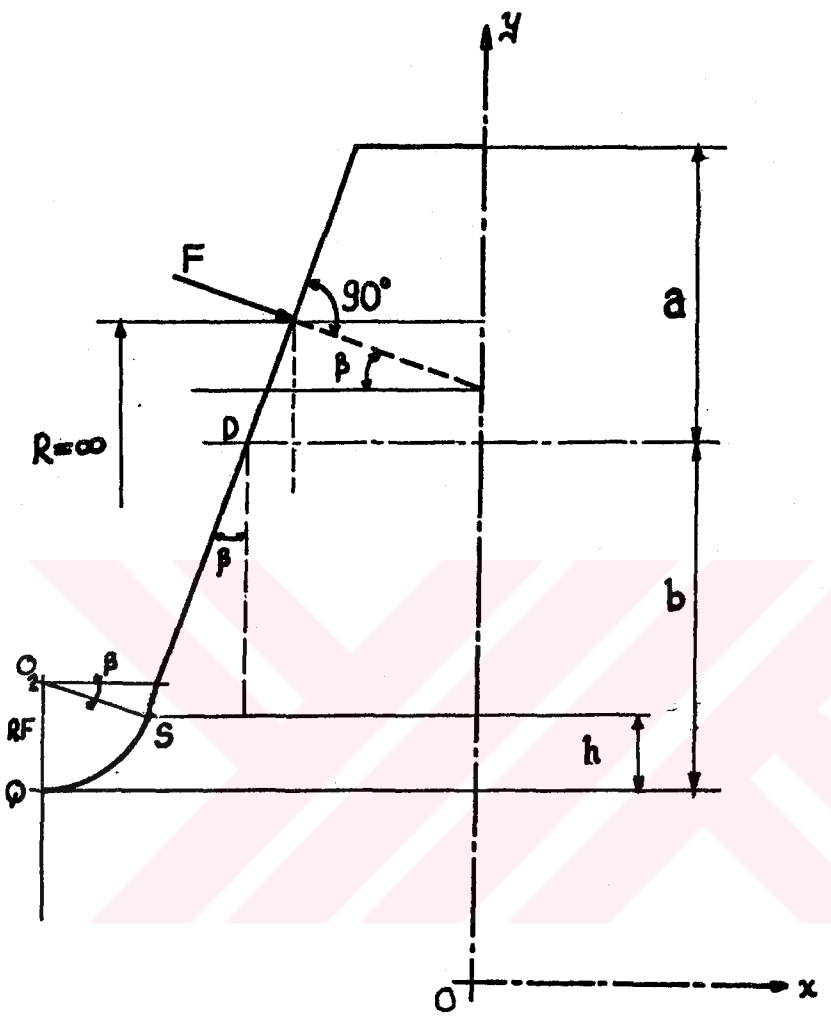

Figure 3.4. Expressions for a Rack

We may imagine a rack as a spur gear having an infinitely large pitch diameter. Therefore the rack has an infinite number of teeth and a base circle which is an infinite distance from the pitch point. The sides of involute teeth on a rack are straight lines making an angle to the line of centers equal to the pressure angle. In Figure 3.4 a tooth of rack is given. In this case the following equations can be written ;

$\beta=\phi$=Pressure angle

Q_y=Rim Thickness (3.11)

$Q_x=O_{2x}$ (3.12)

$O_{2x}=S_x+RF\ Cos\beta$

$O_{2y}=Q_y+RF$

$h=RF(1-Sin\beta)$

$S_y=Q_y+h$ (3.13)

$S_x=(b-h)\ Tan\beta+\frac{\pi m}{2}$ (3.14)

3.3. CONTACT RATIO

When selecting the number of teeth and the size of a mating pair of teeth, it is essential for smooth continuous action that before a pair of teeth goes out of contact, a second pair of teeth enter mesh and assume contact. In Figure 3.5 it will be seen that contact is limited to the distance **a-b** which is determining by the addendum circles of the gears. The initial contact will take place when the flank of the driver comes into contact with the tip of the driven tooth. This occurs at point **a** , where the addendum circle of the driven gear crosses the pressure line. If we now construct tooth profiles through point **a** and draw radial lines from the intersections of these profiles with the pitch circles to the gear centers, we obtain the *angles of approach.*

As the teeth go into mesh, the point of contact will slide up the side of the driving tooth so that the tip of the driver will be in contact just before contact ends. The final point of contact will therefore be where the addendum circle of the driver crosses the pressure line. This is point **b** in Figure 3.5. By drawing another set of tooth profiles through **b**, we obtain the *angle of recess* for each gear

in a manner similar to that of finding the angle of approach. The sum of the angle of approach and the angle of recess for either gear is called the *angle of action.* The line a–b is called the *line of action.* This distance, divided by the base pitch is defined as *the contact ratio.*

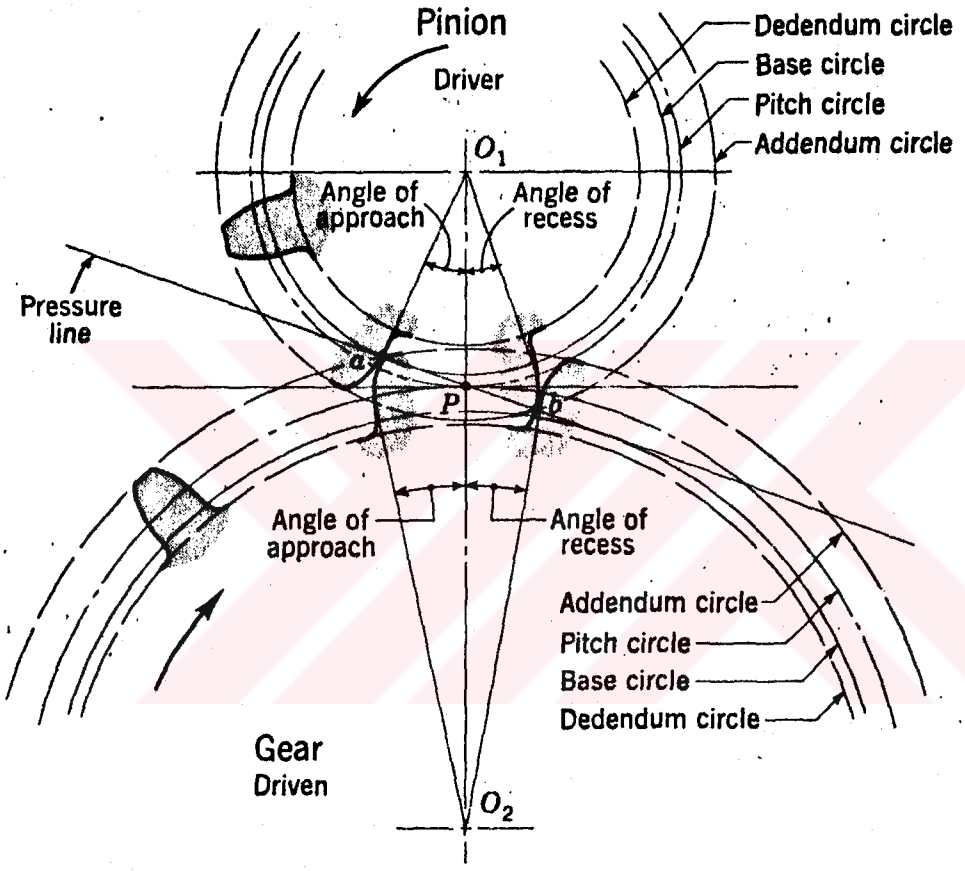

Figure 3.5. Tooth action

$$\varepsilon = \frac{Z}{\pi m \cos\phi} \qquad (3.15)$$

where $Z = \sqrt{(RP_G)^2 - (RB_G)^2} + \sqrt{(RP_P)^2 - (RB_G)^2} - C \sin\phi$

$C = RP_G + RP_P$

The value of ε for a rack can be calculated by using the following equation :

$$\varepsilon=\frac{1}{2\pi}\left[\sqrt{\left(\frac{N+2}{\cos\phi}\right)^2-N^2}-N\tan\phi+\frac{4}{\sin 2\phi}\right] \qquad (3.16)$$

When gears are made accurate enough for the teeth to share load, the tip load condition is not the most critical. In nearly all gear designs, the contact ratio is high enough to put a second pair of teeth in contact when one pair has reached the tip load condition on one member. The worst load condition occurs when a single pair of teeth carry full load.

Gears should not generally be designed having contact ratios less than about 1.20 because inaccuracies in mounting might reduce the contact ratio even more, increasing the possibility of impact between the teeth as well as an increase in the noise level.

3.4. HIGHEST POINT OF SINGLE PAIR CONTACT

Figure 3.6 shows a step-by-step sequence of the events that occur as a pair of teeth go through the mesh sequence. At (a) a pair of teeth have just entered contact. From this point on, they will begin to assume their share of the load. The teeth that are already in mesh have been carrying all of the load. At (b) the previous pair is just leaving mesh. Thus, the entire load is now placed on the pair being observed. The point on the gear where contact is made with the pinion is called *the highest point of single tooth contact.* This pair of teeth will now carrying the full load until the point is reached where the following pair of teeth come into contact and begin to assume their share of the load. Just prior to this point, the pinion tooth is subjected to full load at its highest point of single tooth contact. At (c) the following pair of teeth entering contact and are about to assume their share of th eload. At (d) the subject teeth are leaving mesh.

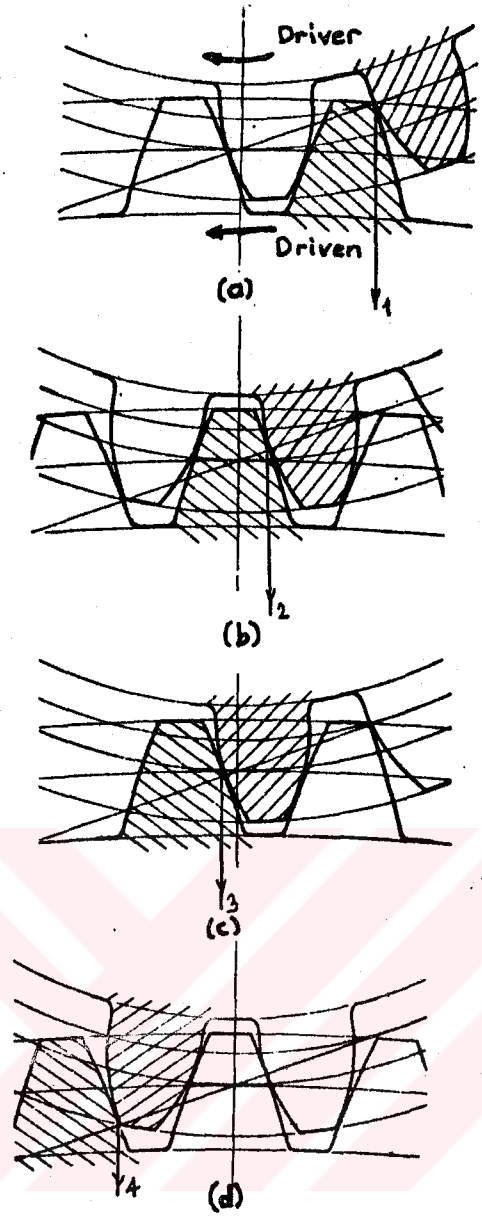

Figure 3.6. Sequence of events of Gear teeth in action

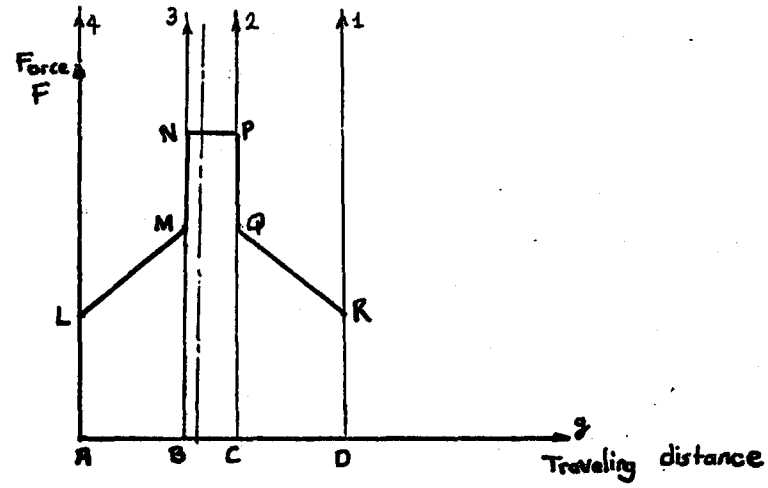

Figure 3.7. Variation of force with traveled distance

When the load is shared by two pairs of teeth, the variations of force F with respect to the traveled distance, g, of the meshing point is strictly linear. In other terms line LM and QR in Figure 3.7, are straight lines, with evidently the same slope since the added force values at two points on LM and QR whose g values shifted must correspond to the total load F. The LMNPQR contour will then be symmetrical with respect to a vertical line if points M and Q have the same ordinate (i.e. force) values.

Moreover, for given F and M values length AB and CD are equal. This can be proved as follows :

For the contact ratio between 1 and 2, load carrying by one pair $(2/\varepsilon-1)$ of the time and load s carrying by two pair $(2-2/\varepsilon)$ of the time [63]. By using Figure 3.7 and these equations ;

$$\frac{BC}{AB+CD}=\frac{\frac{2}{\varepsilon}-1}{2-\frac{2}{\varepsilon}}=\frac{2-\varepsilon}{2\varepsilon-2} \qquad \text{substituting } \varepsilon=\frac{AB}{AC}$$

$$\frac{BC}{AB+CD}=\frac{1-\frac{AD}{AC}}{2\frac{AD}{AC}-1} \qquad \text{where } AD=AB+BC+CD \text{ and } AC=AD-CD$$

$$\text{then} \quad \frac{BC}{AB+CD}=\frac{AB+BC-CD}{2CD}$$

$(AB-CD)(AB+BC+CD)=0$ $\qquad AB+BC+CD=AD$ can not be zero therefore $AB=CD$

The important point here is the determination of the location of the contact point (corresponding point of B) on the tooth profile. This point is named as the highest point of single tooth contact and by drawing a layout of a gear tooth its location is determined as follows ;

From Figure 3.8, it can easily be shown that ;

$$ZB=\sqrt{(RA_0)^2-(RB_0)^2}-\sqrt{(RP_0)^2-(RB_0)^2} \qquad (3.17)$$

$$\text{and} \quad ZC=\pi m \cos\phi-ZB \qquad (3.18)$$

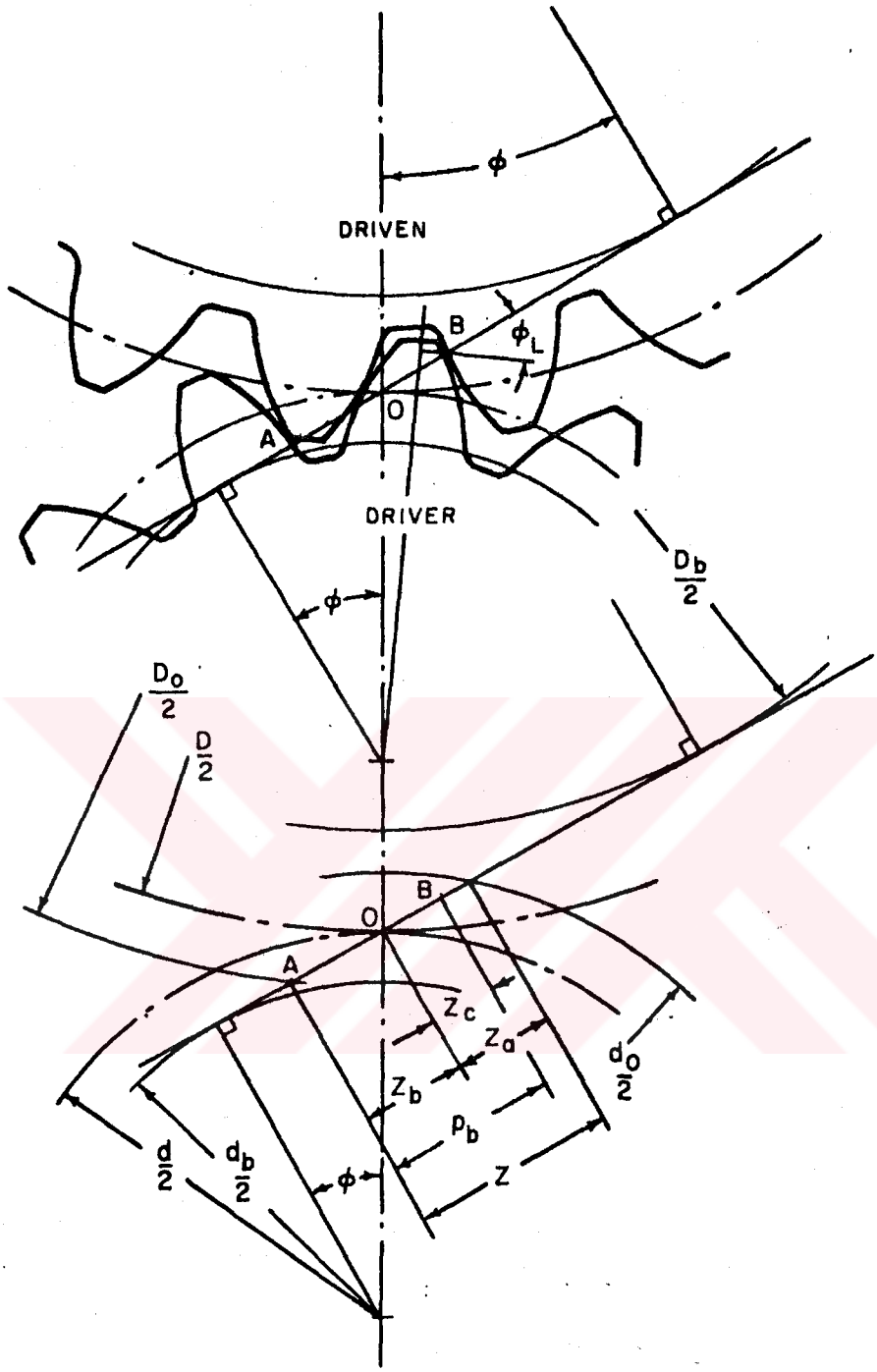

Figure 3.8. Diagram showing highest point of single pair contact in a pair of spur gears.

By using these equations and Figure 3.9 the highest point of single pair contact can be found as ;

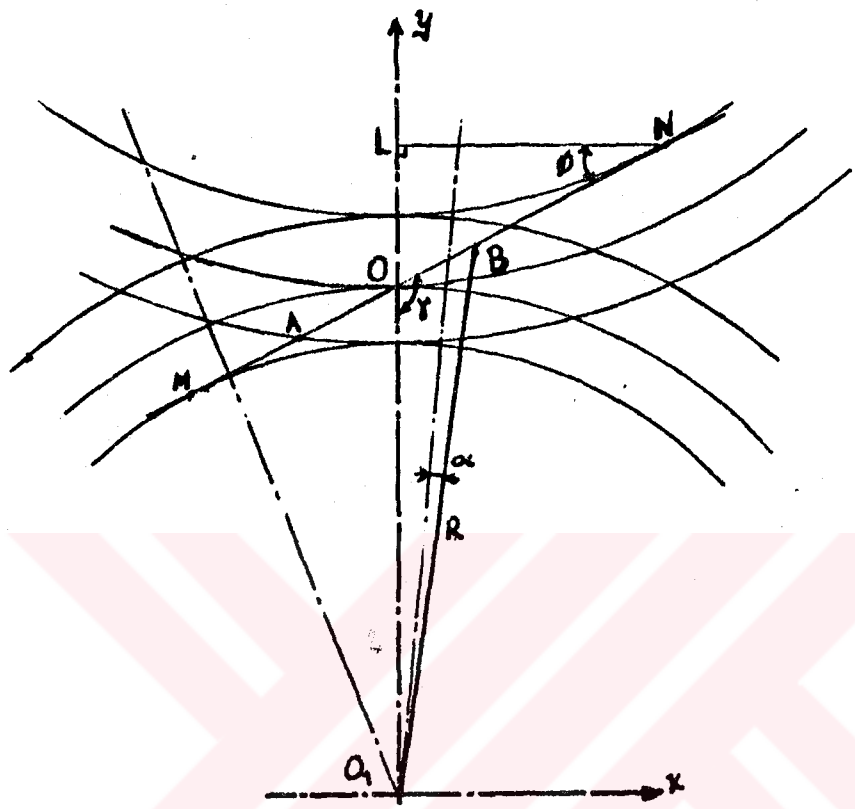

Figure 3.9. Determination of highest point of single tooth contact.

$$OB=ZC$$

By using triangles NOL and O_2BO we can found that

$$R=\sqrt{RP^2+ZC^2+2\,RP\,ZC\,Cos\phi} \qquad (3.19)$$

Angle α can be found by using the involute equations that are given in the preceeding section. The actual coordinates of force point with respect to tooth center is found from the following relations ;

$$XF=R\,Cos\alpha \qquad (3.20)$$

$$YF=R\,Sin\alpha \qquad (3.21)$$

3.5. BEAM STRENGTH OF GEAR TEETH

In the classical approach to the beam strength of the teeth, the gear teeth are considered as cantilever beam.The most severe conditions of loading would be when the full load is carried at the tips of the teeth.On the more accurate gears, the full load will not be carried at the tip points, because with a slight amount of elastic deformation, the load will be shared by a second pair of mating gear teeth. However, when the requirements of weight and size of gears are not critical, a condition that includes the great majority of gears used in machine design, we shall certainly be safe if we assume that the full value of the load is acting at the tip of a single gear tooth.

3.5.1. Lewis Formula

Wilfred Lewis appears to have been the first to use the form factors in a formula for the strength of gear teeth. This formula, which has become the one most widely used appeared in a paper in 1892. This formula is as follows:

$$F = \sigma m b Y \qquad (3.22)$$

where F = safe bending load on gear tooth

σ = safe working stress of material

b = face width of gear

m = module

Y = tooth form factor

3.5.2. Determination of Tooth Form Factor

The tooth form factor Y is obtained by considering the gear tooth as a beam, fixed at one end and loaded at the other. Using graphical approach, form factor is determined as follows ;

$$F=\frac{\sigma bt^2}{bh}$$

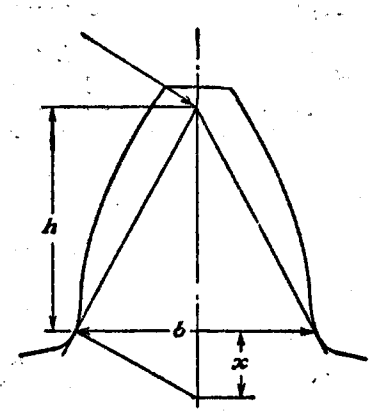

Figure 3.10. Determination of tooth form factor

By using similar triangles of Figure 3.10 ;

$$\frac{x}{t/2}=\frac{t/2}{h}$$

then

$$x=\frac{t^2}{4h}$$

Substituting this value into Equation (3.1);

$$F=\sigma b\frac{2x}{3}=\sigma bm\frac{2x}{3m}=\sigma bmY$$

so that

$$Y=\frac{2x}{3m} \qquad (3.23)$$

This was the method used by Lewis with the load applied at the tip of the tooth rather than the highest point of single pair contact. Also, he ignored the radial component of the normal load and the weakest section that was used by him, is not the actual one, it is only an approximation.

3.5.3. Stress Concentration at Fillet

Whenever,there is a rapid increase of section in a stressed body made of elastic material,there will be an increased local stress concentration at the region of increase of section. The intensity of this stress concentration depends largely upon the rate of section. Thus the actual maximum local stresses at the root of a loaded gear tooth are larger than the average stresses as determined by any bending formula such as the Lewis equation.

Photoelastic studies of the stress concentrations at the roots of gear teeth have been made by several investigators. Similar studies have been made upon the effects of the size of fillets on the stress concentrations in test bars. These results have been compared with the results on similar metal bars subjected to fatigue tests. Because of the local yielding and work hardening of the softer materials, and their apparently lower values of the stress concentration, gears made of such materials as cast iron, bronze, and soft steel would use a lower stress concentration factor than those obtained from photoelastic tests. For gears made of hardened steel, however, the full value of the photoelastic stress concentration factors should be used.

Many investigators have noted that the stress concentration at the fillet of the nonloaded or compression side of the gear tooth are larger than those on the loaded or tension side of the tooth. Some claim is made that there is no fatigue under compressive stresses, yet the great majority of broken gear teeth show the fracture extending from the fillet on the compression side into the gear blank and up and out on the loaded or tension side of the tooth above the fillet,as indicated in Figure 3.11.

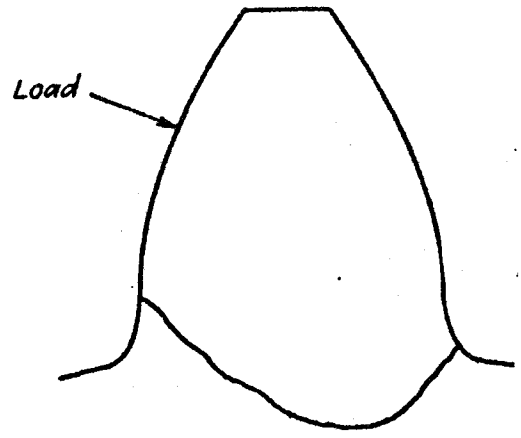

Figure 3.11. Typical Tooth Fracture

3.5.3.1. Lewis Equation With Fillet Stress Concentration Factor

When a suitable working stress has been selected, the limiting beam load for gear tooth can be computed from the Lewis equation and the fillet stress concentration factor. This limiting beam load should be greater than the dynamic load to provide a margin of safety. Such a margin will be a measure of the additional load that can be carried. Some margin of safety is always desirable. With spur gears, a broken tooth means a failure of the gear drive. This margin of safety should be enough, at least, to cover the probable increase of error in action because of wear. The softer or more plastic materials of the gears may be, the greater the chances are that the error in action will increase with continued service.

A theoretical, or geometric, stress concentration factor K_t is used to relate the actual maximum stress at the discontinuity to the nominal stress. The factor is defined by the equations

$$K_t=\frac{\sigma_{max}}{\sigma_0} \qquad (3.24)$$

The subscript t in K_t means that this stress concentration factor depends for its value only on the *geometry* of the part. That is, the particular material used has no effect on the value of K_t. This is why it is called a *theoretical* stress concentration factor.

The Lewis equation may be modified to include the fillet stress concentration factor (K_t) as follows:

$$F=\frac{\sigma_m b Y}{K_t} \qquad (3.25)$$

3.5.3.2. Equations of Dolan and Broghamer

In an attempt to improve upon the well known Lewis equation for gear tooth, Dolan and Broghamer devised empirical equations for the stress concentration factors at the tensile fillets of gear teeth that accorded with their experimental findings within an accuracy of 3 %. These equations, based on the assumption that the load is carried entirely by one tooth only, are as given below :

$$K_t=\left(\frac{t}{h}\right)^{0.4}\left(\frac{t}{RF}\right)^{0.2}+0.22 \qquad \text{for } \phi=14\frac{1}{2} \text{ degree} \qquad (3.26)$$

$$K_t=\left(\frac{t}{h}\right)^{0.45}\left(\frac{t}{RF}\right)^{0.15}+0.18 \qquad \text{for } \phi=20 \text{ degree} \qquad (3.27)$$

where t is the tooth thickness weakest section, h is the height from the weakest section to the point of intersection of the load line of action and the tooth centerline, and r is the tooth fillet radius.

Although the above equations provide valuable information on the stress concentrations of gear teeth, they are still not widely used in gear design. This is because of the graphical analysis required in making a layout of a gear tooth, and then applying the Lewis method of construction, or the trial method of construction, for the location of t and h, before it can be made possible to determine K_t from above equations.

CHAPTER 4

APPLICATION OF FEM TO THE STRESS ANALYSIS

4.1. INTRODUCTION

In this chapter,the application of FEM to any plane structure is discussed. Section 4.2 gives the general steps in the solution to any stress analysis problem by the FEM. In section 4.3 the application of FEM to a plane structure that is broken into triangular elements is given.

4.2. HOW THE METHOD WORKS

In a continuum problems of any dimension, the field variable (whether it is pressure, temperature, displacement, stress, or some other quantity) possesses infinitely many values because it is a function of each generic point in the body or solution region. Consequently, the problem is one with an infinite number of unknowns. The finite element discretization procedures reduce the problem to one of a finite number of unknowns by dividing the solution region into elements and by expressing the unkown field variable in terms of assumed approximating functions within each element.The approximating functions (sometimes called *interpolation functions*) are defined in terms of the values of the field variables at specified points called *nodes* or *nodal points.* Nodes usually lie on the element boundaries where adjacent elements are considered to be connected. In addition to boundary nodes, an element may also have a few interior nodes. The nodal values of the field variable and the interpolation functions for the elements completely define the behavior of the field variable within the elements. For the finite element representation of

a problem, the nodal values of the field variable become the new unknowns. Once these unknowns are found, the interpolation functions define the field variable throughout the assemblage of elements.

Clearly, the nature of the solution and the degree of approximation depend not only on the size and number of the elements used, but also on the interpolation functions selected. As one would expect, we cannot choose functions arbitrarily because certain compatability conditions should be satisfied. Often functions are choosen so that the field variable or its derivatives are continuous across adjoining element boundaries.

Thus far, we have briefly discussed the concept of modeling and an arbitrarily shaped solution region with an assebmlage of discrete elements; and we have pointed out that interpolation functions must be defined for each element. We have not yet mentioned, however, an important feature of the FEM which sets it apart from other approximate numerical methods. That feature is the ability to formulate solutions for individual elements before putting them together to represent the entire problem. This means, for example, that if we are treating a problem in stress analysis, we can find the force-displacement or stiffness characteristics of each individual element and then assemble the elements to find the stiffness of the whole structure. In essence,a complex problem reduces to considering a series of greatly simplified problems.

Another advantage of the FEM is the variety of ways in which one can formulate the properties of individual elements. There are basically four different approaches. The first approach to obtaining element properties is called the *direct approach* because its origin is traceable to the direct stiffness method of structural analysis. Although the direct approach can be used only for relatively simple problems,it is easiest to understand when meeting the FEM for the first time. The direct approach also suggests the need for matrix algebra in dealing with the finite element equations.

Element properties obtained by the direct approach can also be determined by the more versatile and more advanced *variational approach.* The variational approach relies on the calculus of variations and involves extremizing a *functional.* For problems in solid mechanics, the functional turns out to be the potential energy, the complementary potential energy, or some derivative of these. Whereas the direct approach can be used to formulate element properties for only the simplest element shapes, the variational approach can be employed for both simple and sophisticated element shapes.

A third and even more versatile approach to deriving element properties has its basis entirely in mathematics and is known as the *weighted residuals approach.* The weighted residuals approach begins with the governing equations of the problem and proceeds without relying on a functional or a variational statement. This approach is advantageous because it thereby becomes possible to extend the FEM to problems where no functional is available. For some problems, we do not have a functional (either because one may not have been discovered or because one does not exist.

A fourth approach relies on the balance of thermal and/or mechanical energy of a system. The *energy balance approach* (like the weighted residuals approach) requires no variational statement and hence broadens considerably the range of possible applications of the FEM.

Regardless of the approach used to find the element properties, the solution of a continuum problem by the FEM always follows an orderly step-by-step process. To summarize in general terms how the finite element method works, these steps can be listed;

4.2.1. *Discritize the continuum*

The first step is to divide the continuum or solution region into elements. In example of Figure 4.1, the turbine blade has been divided into triangular elements which might be used to find the temperature

distribution in the blade. A variety of element shapes may be used, and, with care, different element shapes may be employed in the same solution region. Indeed, when analyzing an elastic structure that has different types of components such as plates and beams, it is not only desirable but also necessary to use different types of elements in the same solution. Although the number and the type of elements to be used in a given problem are matters of engineering judgment, the analyst can rely on the experience of others for guidelines.

4.2.2. *Select interpolation functions*

The next step is to assign nodes to each element and then choose the type of interpolation function to represent the variation of the field variable over the element. The field variable may be a scalar, a vector, or a higher-order tensor. Often, although not always, polynomials are selected as interpolation functions for the field variable because they are easy to integrate and differentiate. The degree of the polynomial chosen depends on the number of nodes assigned to the element, the nature and number of unknowns at each node, and certain continuity requirements imposed at the nodes and along the element boundaries. The magnitude of the field variable as well as the magnitude of its derivatives may be the unknowns at the nodes.

4.2.3. *Find the element properties*

Once the finite element model hasa been established (that is, once the elements and their interpolation functions have been selected), we are ready to determine the matrix equations expressing the properties of the individual elements. For this task, we may use one of the four approaches just mentioned : the direct approach, the variational approach, the weighted residual approach, or the energy balance approach. The variational approach is often the most convenient, but for any application the approach used depends entirely on the nature of the problem.

4.2.4. *Assemble the element properties to obtain the system equations*

To find the properties of the overall system modeled by the network of elements, we must assemble all the element properties. In other words, we must combine the matrix equations expressing the behavior of the elements and form the matrix equations expressing the behavior of the entire solution region or system. The matrix equations for the system have the same form as the equations for an individual element except that they contain many more terms because they include all nodes.

The basis for the assembly procedure stems from the fact that, at a node where elements are interconnected, the value of the field variable is the same for each element sharing that node. Assembly of the element equations is a routine matter in finite element analysis and is usually done by electronic computer.

Before the system equations are ready for solution, they must be modified to account for the boundary conditions of the problem.

4.2.5. *Solve the system equations*

The assembly process for the preceeding step gives a set of simultaneous equations which we can solve to obtain the unknown nodal values of the field variable. If the equations are linear, we can use a number of standard solution techniques. If the equations are non-linear, the solution is more difficult to obtain. There are several approaches to non-linear problems.

4.2.6. *Make additional computations if desired*

Sometimes we may want to use the solution of the system equations to calculate other important parameters. For example, in a

fluid mechanics problem such as the lubrication problem, the solution of the system equations gives the pressure distribution within the system. From the nodal values of the pressure, we may then calculate velocity distributions and flows or perhaps shear stresses if these are desired.

4.3. TRIANGULAR ELEMENTS

4.3.1. Displacement Functions For Triangular Elements

Consider an elastic plate that is cut into triangles which are then connected together at the nodes only, as in Figure 4.1a. If a load is applied as in Figure 4.1b, it would be expected that the deformations might give shapes such as those shown. That is, gaps might open up along the edges and more deformation than in the original uncut plate would be expected. This must not be allowed, as the system is influenced by such behaviour. By connecting the triangles at the corners, we ensure that the displacements of all triangles joining at any node are the same at that one point. This is expressed by saying that the displacements are compatible at the nodes, which is the case in the original plate. However, at neighboring points on an edge, the displacements in Figure 4.1b are not necessarily the same. If the plate is to behave as it did before it was partitioned into triangles, the compatibility of displacements along the edges, as well as at the nodes, must be assured. This problem did not arise in the pin-jointed structure and we will deal with it later.

Consider a triangle such as that of Figure 4.2. The triangle has been given displacements δ and the calculation of the force components in $\mathbf{f}$ is desired. This could be done if the stiffness matrix $\mathbf{K}$, is known by

$$f = K\,\delta \qquad (4.1)$$

Therefore, determination of the 36 values (3 nodes on the corners of a triangle with two-degrees of freedom gives 6X6 matrix) of in $\mathbf{K}$ is necessary. Begin with by assuming displacement functions u and v that

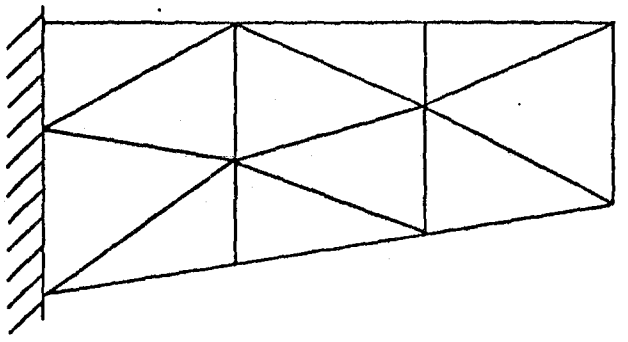

(a) unloaded

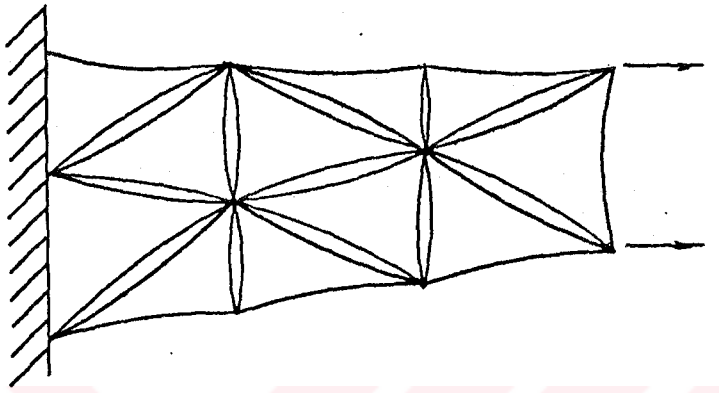

(b) loaded

Figure 4.1. Deformation of elastic plate under load

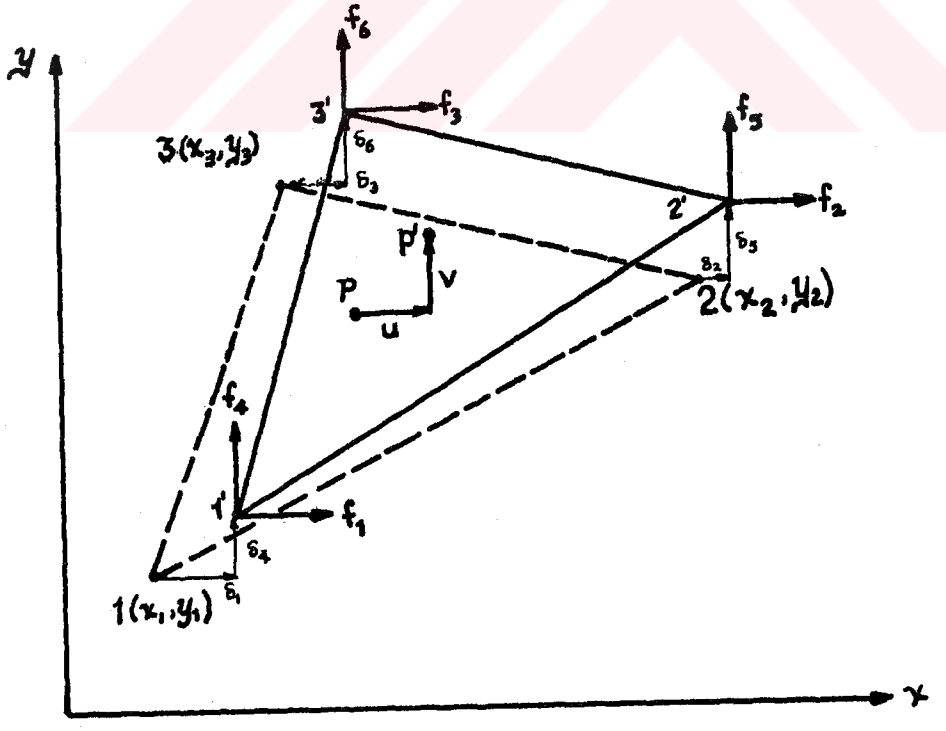

Figure 4.2 Deformation of a Triangular Element

would give the horizontal and vertical displacements at any point $p(x,y)$ in the triangle. Invariably, in the FEM the displacement functions are taken as polynomials. Since the horizontal displacements are known at only three points, that is the nodes, no more than three coefficients in the polynomial can be included and hence the highest order expression that we should attempt is

$$u = a_1 + a_2 x + a_3 y$$

similarly choose

$$v = a_4 + a_5 x + a_6 y$$

or,

$$\begin{Bmatrix} u \\ v \end{Bmatrix} = \begin{bmatrix} 1 & x & y & 0 & 0 & 0 \\ 0 & 0 & 0 & 1 & x & y \end{bmatrix} a \qquad (4.2)$$

When **a** is known, these expressions will give displacements at all locations in the plate. But it is known that

$$u_{x=x_1} = \delta_1 = [\,1 \;\; x \;\; y \;\; 0 \;\; 0 \;\; 0\,]$$

The other five known displacements lead to similar expressions. These can be written as follows :

$$\begin{bmatrix} 1 & x & y & 0 & 0 & 0 \\ 1 & x & y & 0 & 0 & 0 \\ 1 & x & y & 0 & 0 & 0 \\ 0 & 0 & 0 & 1 & x & y \\ 0 & 0 & 0 & 1 & x & y \\ 0 & 0 & 0 & 1 & x & y \end{bmatrix} \begin{bmatrix} a_1 \\ a_2 \\ a_3 \\ a_4 \\ a_5 \\ a_6 \end{bmatrix} = \begin{bmatrix} \delta_1 \\ \delta_2 \\ \delta_3 \\ \delta_4 \\ \delta_5 \\ \delta_6 \end{bmatrix} \qquad (4.3)$$

or,

$$A\,a = \delta \qquad (4.4)$$

The solution for the unknown coefficients is given by

$$a = A^{-1}\,\delta \tag{4.5}$$

The inverse can be obtained by operating directly on A, but it is more economical to take the advantage of the special properties of A and partition it into .

$$A = \begin{bmatrix} \bar{A} & \emptyset \\ \emptyset & \bar{A} \end{bmatrix}$$

and inverting only $\bar{A}$, which in this case is such a simple operation that it can be done by hand. Then

$$A^{-1} = \begin{bmatrix} \bar{A}^{-1} & \emptyset \\ \emptyset & \bar{A}^{-1} \end{bmatrix} \tag{4.6}$$

The coefficients in (4.2) can now be eliminated by substituting from (4.5) to get

$$\begin{bmatrix} u \\ v \end{bmatrix} = \begin{bmatrix} 1 & x & y & \emptyset & \emptyset & \emptyset \\ \emptyset & \emptyset & \emptyset & 1 & x & y \end{bmatrix} A^{-1}\,\delta \tag{4.7}$$

We will know pause to examine the implications of our choice of displacement functions. Referring to Figure 4.2, let us consider that all coordinates of nodes and all nodal displacements are known, then in (4.7) all coefficients in the polynomials are known. If we consider points on one side, say 1-2. the x and y in the polynomial are linearly related so that for points at varying distances from 1 toward 2 the u varies linearly as does also the v. Taking components of displacement normal and tangential to side 1-2, these also vary linearly, the constants in the linear function being determined by the displacements of nodes 1 and 2. On both sides of the interface 1-2, the displacements are determined by

the same nodal diplacements; hence adjacent points on opposite sides of the interface will have identical normal and tangential displacements. Therefore, at all points along the imaginary parting line 1-2 there is no relative motion that would either open a crack or cause relative sliding. This means that compatible displacements at the nodes, combined with the choosen displacement functions, ensure compatibility along all edges of triangles and the gaps between adjacent triangles, as shown in Figure 4.1b do not occur.

4.3.2. Strains in a Triangular Element

The displacement functions is the assumed form are not of much use to us.However they will lead us to a determination of strains and thence to our real objective ,stress.

In the x, y plane strain and displacement are related by

$$\varepsilon_{xx}=\frac{\partial u}{\partial x}$$

$$\varepsilon_{yy}=\frac{\partial v}{\partial y}$$

$$\varepsilon_{xy}=\frac{\partial u}{\partial y}+\frac{\partial v}{\partial x}$$

which can be verified by reference to a text on the theory of elasticity. these expressions can be input into matrix form

$$\varepsilon = \begin{bmatrix} \varepsilon_{xx} \\ \varepsilon_{yy} \\ \varepsilon_{xy} \end{bmatrix} = \begin{bmatrix} \frac{\partial}{\partial x} & 0 \\ 0 & \frac{\partial}{\partial y} \\ \frac{\partial}{\partial y} & \frac{\partial}{\partial x} \end{bmatrix} \begin{bmatrix} u \\ v \end{bmatrix}$$

When displacements are substituted from (4.7) this becomes

$$\varepsilon = \begin{bmatrix} \frac{\partial}{\partial x} & 0 \\ 0 & \frac{\partial}{\partial y} \\ \frac{\partial}{\partial y} & \frac{\partial}{\partial x} \end{bmatrix} \begin{bmatrix} 1 & x & y & 0 & 0 & 0 \\ 0 & 0 & 0 & 1 & x & y \end{bmatrix} A^{-1} \delta$$

Since there are no variables in A^{-1} nor in δ, the differentiations have no effect on these quantities, and the differential operations lead to

$$\varepsilon = \begin{bmatrix} 0 & 1 & 0 & 0 & 0 & 0 \\ 0 & 0 & 0 & 0 & 0 & 0 \\ 0 & 0 & 1 & 0 & 1 & 0 \end{bmatrix} A^{-1} \delta$$

Let

$$B = \begin{bmatrix} 0 & 1 & 0 & 0 & 0 & 0 \\ 0 & 0 & 0 & 0 & 0 & 0 \\ 0 & 0 & 1 & 0 & 1 & 0 \end{bmatrix}$$

then

$$\varepsilon = B A^{-1} \delta \qquad (4.8)$$

Equation (4.8) gives the strains at any point p(x,y) in the triangular element. But inspection of the terms in the equation shows that x and y do not appear and that all entries are constants. Consequently, the three strains have the same values at all points in the triangle. For this reason, the triangle is often referred to as the *constant strain triangle* although it might equally well be described as a *linearly varying displacement triangle.*

4.3.3. Stress in a Triangular Element

In elementary mechanics of materials, the equations for strain in an isotropic material were established as

$$\varepsilon_{xx}=\frac{1}{E}\sigma_{xx}-\frac{\nu}{E}\sigma_{yy}$$

$$\varepsilon_{yy}=-\frac{\nu}{E}\sigma_{xx}+\frac{1}{E}\sigma_{yy}$$

$$\varepsilon_{xy}=\frac{2(\nu+1)}{E}\sigma_{xy}$$

which may be expressed in matrix form as

$$\begin{bmatrix}\varepsilon_{xx}\\ \varepsilon_{yy}\\ \varepsilon_{xy}\end{bmatrix} = \frac{1}{E}\begin{bmatrix}1 & -\nu & 0\\ -\nu & 1 & 0\\ 0 & 0 & 2\ 1-\nu\end{bmatrix}$$

The equations for stress can be obtained from these by inversion which gives

$$\begin{bmatrix}\sigma_{xx}\\ \sigma_{yy}\\ \sigma_{xy}\end{bmatrix} = \frac{E}{1-\nu^2}\begin{bmatrix}1 & \nu & 0\\ \nu & 1 & 0\\ 0 & 0 & \frac{1-\nu}{2}\end{bmatrix}\begin{bmatrix}\varepsilon_{xx}\\ \varepsilon_{yy}\\ \varepsilon_{xy}\end{bmatrix} \qquad (4.9)$$

Let

$$D = \frac{E}{1-\nu^2}\begin{bmatrix}1 & \nu & 0\\ \nu & 1 & 0\\ 0 & 0 & \frac{1-\nu}{2}\end{bmatrix} \qquad (4.10)$$

then $\sigma = D B A^{-1} \delta$ (4.11)

This equation enables us to calculate the stresses in a triangular element provided we have the elastic properties, the coordinates of the corners, and the displacemens of the corners. It is observed that there are no variables in the right hand side of (4.11) and hence the stresses are constant throughout the element.

4.3.4. Stiffness of Triangular Element

Imagine that the element in Figure 4.2 has been given the displacements δ and we would like to be able to determine the forces f necessary to hold the element in the strained state. This could be done if we knew K, the stiffness matrix in

$$f = K \delta$$

In the state described above, the existing stresses are given by (4.11). Let us superimpose small virtual displacements δ^* on the existing configuration. The virtual displacements must be small enough so that the forces do not change significantly during the displacement. The work done by the forces is then given by

$$w_E = \delta_1^* f_1 + \delta_2^* f_2 + \ldots\ldots + \delta_6^* f_6 = \delta^{*T} f \quad (4.12)$$

During the virtual displacement the strain is given by (4.8) as

$$\varepsilon^* = B A^{-1} \delta^* \quad (4.13)$$

The stress, given by (4.11), which is substentially constant, does work during the virtual strain of an amount that can be calculated for an incremental volume as

$$dw_1 = \varepsilon_{xx}^* \sigma_{xx}\, dv + \varepsilon_{yy}^* \sigma_{yy}\, dv + \varepsilon_{xy}^* \sigma_{xy}\, dv = \varepsilon^{*T} \sigma\, dv$$

Substituting from (4.11) and (4.13) the above expression becomes

$$dw_1=[\,B\,A^{-1}\delta^{*T}]\,D\,B\,A^{-1}\delta\,dv=\delta^{*T}[A^{-1}]^T B^T DBA^{-1}\delta dv$$

In the whole element, the internal work done is

$$w_1=\int_{vol}\delta^{*T}[A^{-1}]^T B^T DBA^{-1}\delta dv$$

Since all quantities in the matrices are constant, the integration needs to be done only on dv which gives the volume of the element, hence

$$w_1=\delta^{*T}[A^{-1}]^T B^T DBA^{-1}\delta\ vol.$$

Since there is no loss of energy in this process, the external energy can be equated to the internal energy giving

$$\delta^{*T}f=\delta^{*T}[A^{-1}]^T B^T DBA^{-1}\delta\ vol.$$

which leads to

$$f=[A^{-1}]B^T DBA^{-1}vol.$$

This is of the same form as (4.1) with

$$K=[A^{-1}]^T B^T DBA^{-1}vol. \qquad (4.14)$$

Every term on the right side of (4.14) is known, so we can calculate the stiffness matrix. For the particular case under consideration, we could work a general solution to all triangular element stiffnesses. In practice it is better to generate the stiffness of each element from (4.14) as it is needed since the programming required to fill in K directly is quite tedious.

4.3.5. Stresses in an In-Plane Loaded Plate

As the stiffness of each triangular element, K, is determined it can be added to the general stiffness matrix K^1. When all triangles in a plate have been considered, the K^1 matrix will represent the total stiffness of the plate in

$$\bar{F} = \bar{K}^1\,\bar{U}$$

Hereafter the subscript, ^{1}, will be omitted for simplicity, the context being sufficient to indicate which stiffness is being referred to. Thus the general stiffness equation becomes

$$F = K\,U$$

For a loaded plate with a given supporting system, part of the F and part of the U components are known. There is a correspondence between knowns and unknowns in F and U such that for any unknown component of F corresponds to same component of known U or vice versa. The practical method of solution is that of using ficticious components of force in place of the unkowns, makes some change in K, and solves as though all the U components are unknown. Let us say that U^1 is a known component. Then a ficticious component is put into the force vector given by

$$F^1 = c\,K^{11}\,U^1$$

where c is a large number.(In practice, $c = 10^{12}$ is satisfactory.)

The stiffness matrix is changed by substituting cK^{11} for K^{11}. The ^{1}th equation is now treated in the same way as all the others, the changes being such that they ensure that the equations when solved will give the original known value for U^1. By treating each row that contains a known U component in this way, the problem is changed to one in which all the F components have numerical values and all the U components are treated as unknowns. Solving this classical problem will give all values of U. A simple substitution of the known U into force equation using the original unmodified K gives all F components, some of which have not been known up to this point and others, that were known, are recalculated. A comparison of these components with the original known components serves as a check on the process. With U determined, the components can be selected for substitution into (4.11) and thus the stress in any element obtained.

CHAPTER 5

COMPUTER AIDED EVALUATION OF GEAR TOOTH STRESSES

5.1. INTRODUCTION

This chapter is devoted to the explanation of the automated method for the evaluation of the gear tooth stresses.

In section 5.2 the computer program and its subroutines for different functions are explained. The results obtained by using this program with several runs are discussed in section 5.3.

5.2. COMPUTER PROGRAM

The method described in chapter 4 have been programmed to solve the gear tooth stresses. The flowchart of the program is given in Figure 5.1.

The models chosen in this study are explained first and than the functions of each subroutine shown in Figure 5.1 are to be discussed in the following subsections.

5.2.1. Modeling of Structure

Finite Element Analysis depends on the construction of a model that divides a component into simple standard shapes or elements, corners, and in some instances midpoints, of these element sides are the locations known as nodes or grid points where deflections are calculated through use of known stiffness properties, applied loads and boundary conditions.

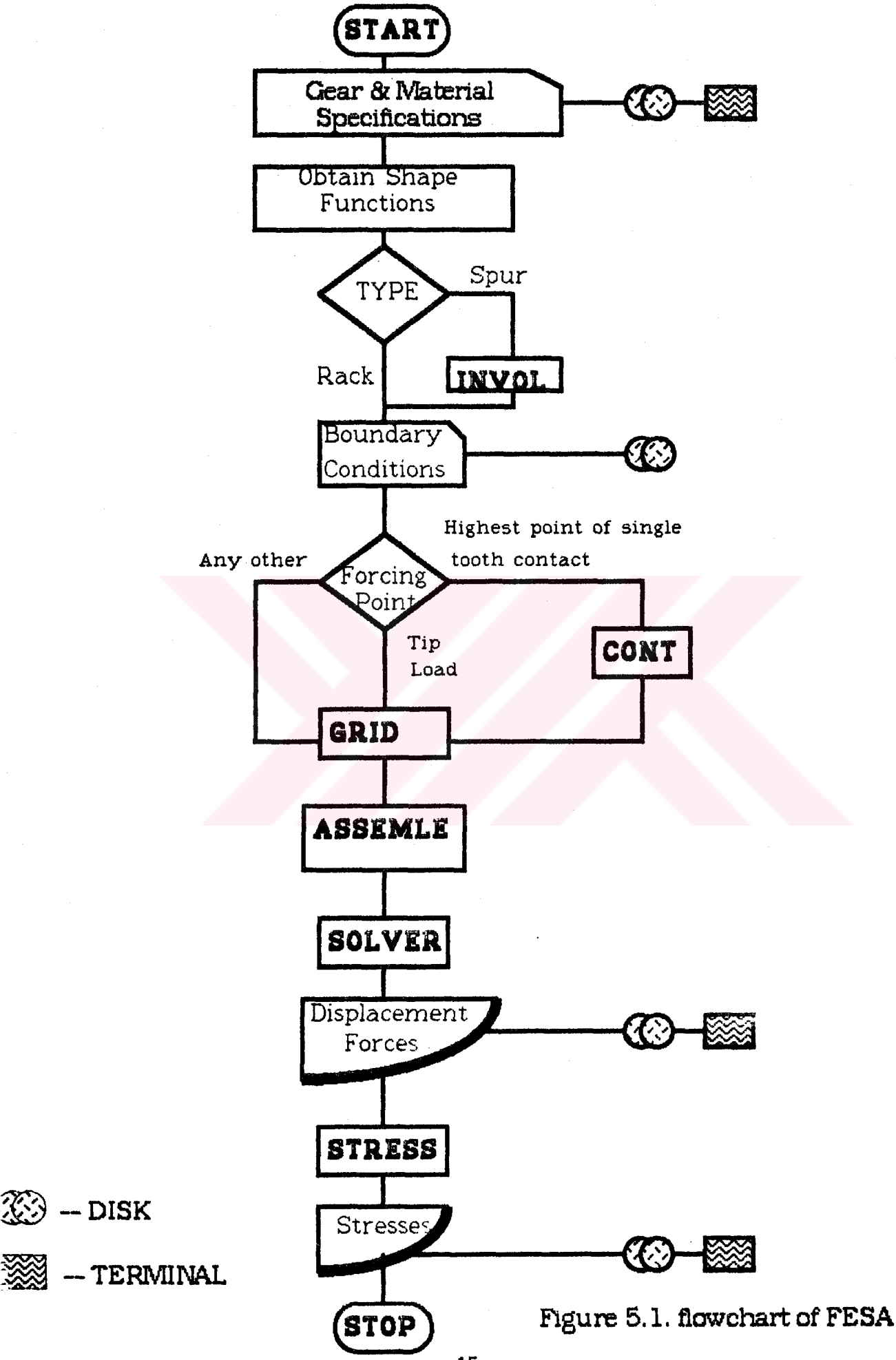

Figure 5.1. flowchart of FESA

A model must accurately represent the stiffness, and provide necessary conditions for application of equivalent loadings and displacement constraints. The model must also have sufficient detail in areas of high stress. Because many alternative ways exist for dividing a model into elements the modeling process can be confusing to a novice.

Before a model is prepared, the actual physical structure should be studied to determine the load and how it is distributed on the part. Also, a determination should be made with regard to how the structure is constrained as well as the directions in which the component is free to move.

It may be possible at this stage to estimate the areas of highest stress, and to locate those portions of the model which require the greatest detail.

Accuracy of the model depends on the types of elements used, the density and size of elements, and distorsion of the elements from their ideal shapes.

In analysis of gear tooth stresses many models were used. Aida and Terauchi [64] used conformal mapping, the convex boundary line of a half-plane was transformed into the horizontal boundary line of a corresponding half plane as in Figure 5.2.

T. Tobe,M. Kato and K. Inoue [58] used a model like in Figure 5.3. Cemil Bagci [65] used a model as in Figure 5.4. Due to physical structure of spur gear, Bagci's approach is better. But not necessary to use three teeth in calculations, because of the computing time, storage capacity and also same results can be obtained by using only one tooth. This was shown by G. Chabert, T. Dang Tran and R. Mathis [57] in their study. Their model is shown in Figure 5.5.

Additionally, in Figures 5.6 and 5.7 two different finite element models of spur gear tooth suggested in Refs.[66,62].

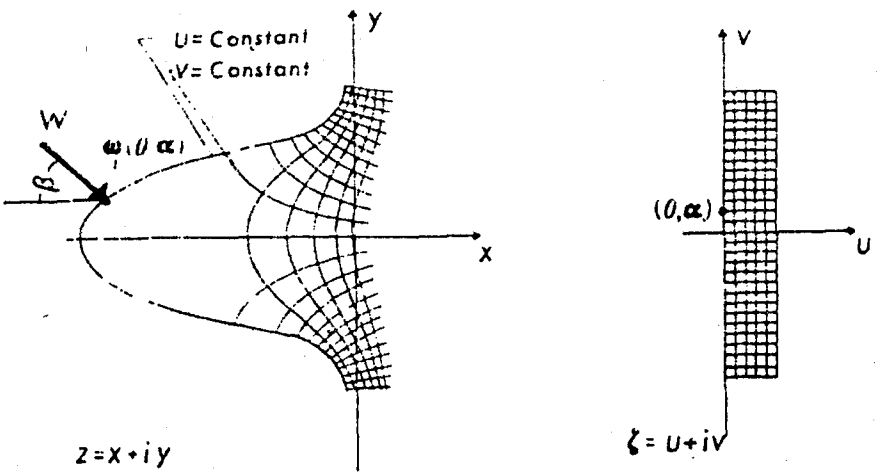

Figure 5.2. The FEM model of spur gear used in Ref.[64]

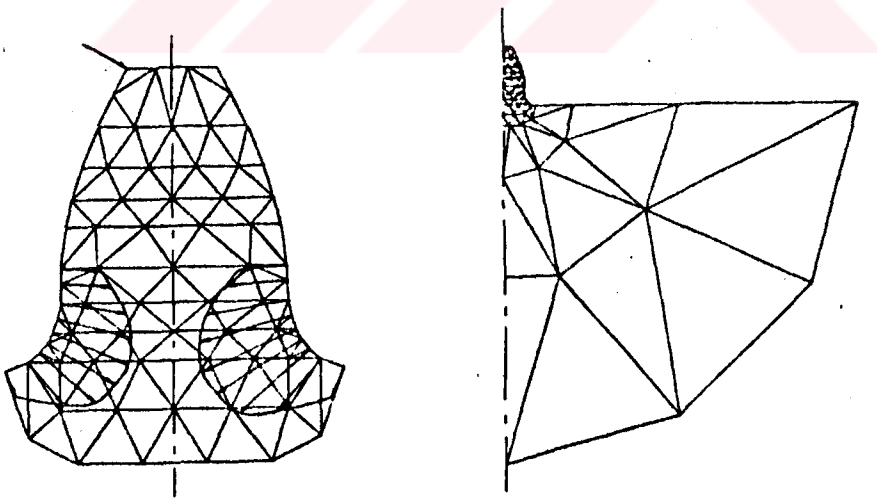

Figure 5.3. The model used in Ref.[58]

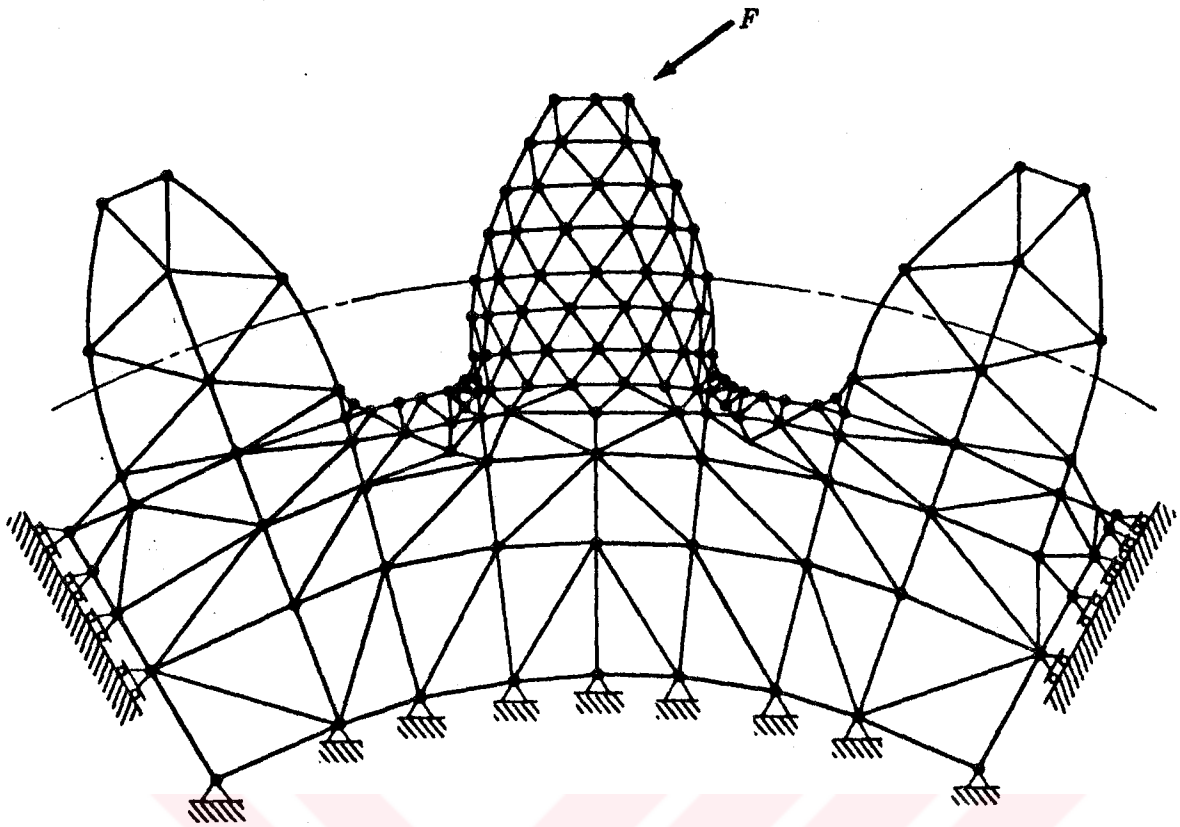

Figure 5.4. The model used in Ref.[65]

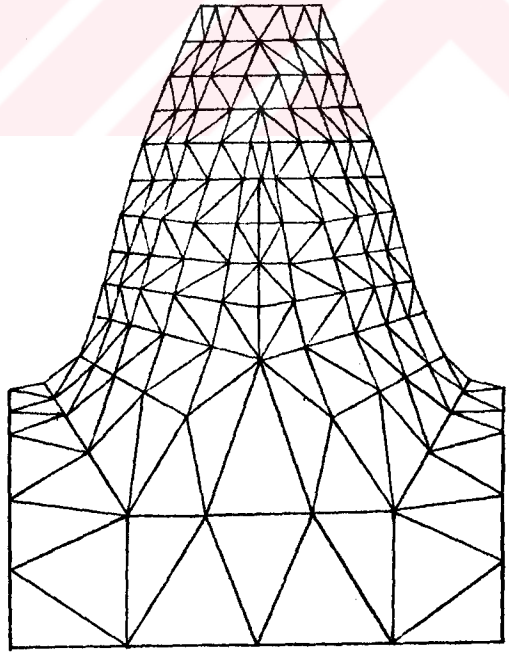

Figure 5.5. The model used in Ref.[57]

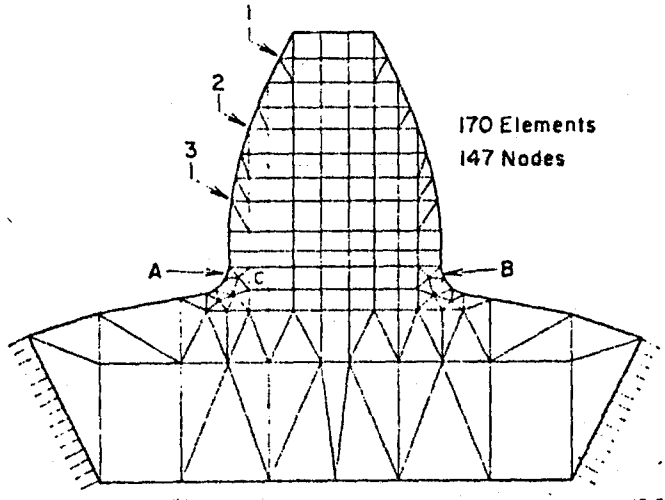

Figure 5.6. FEM model of spur gear used in Ref.[66]

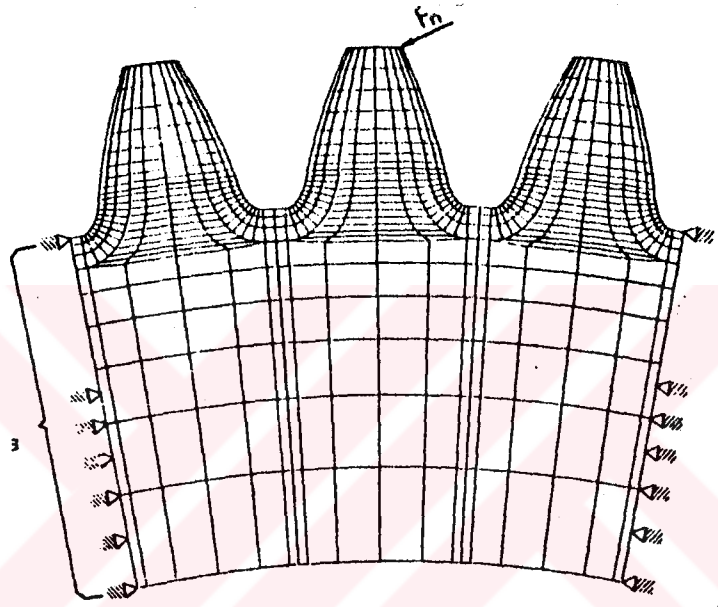

a) support on both sides

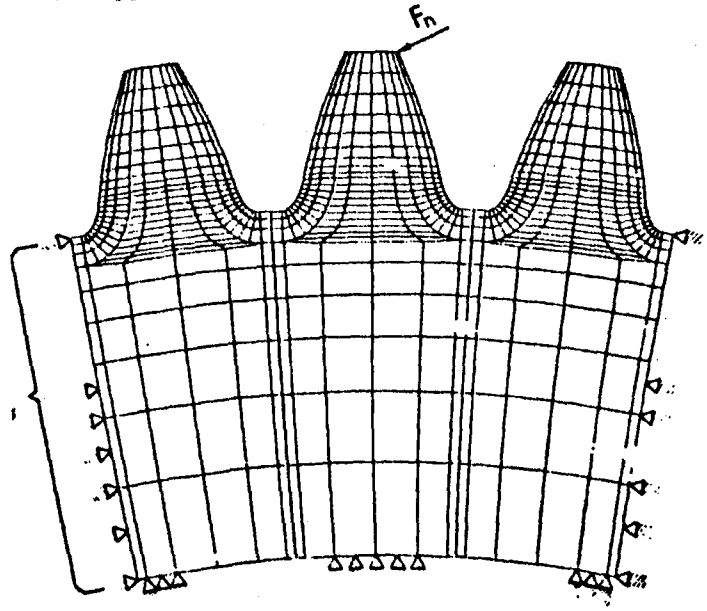

b) support on both sides and along the base

Figure 5.7. FEM model used in Ref.[62]

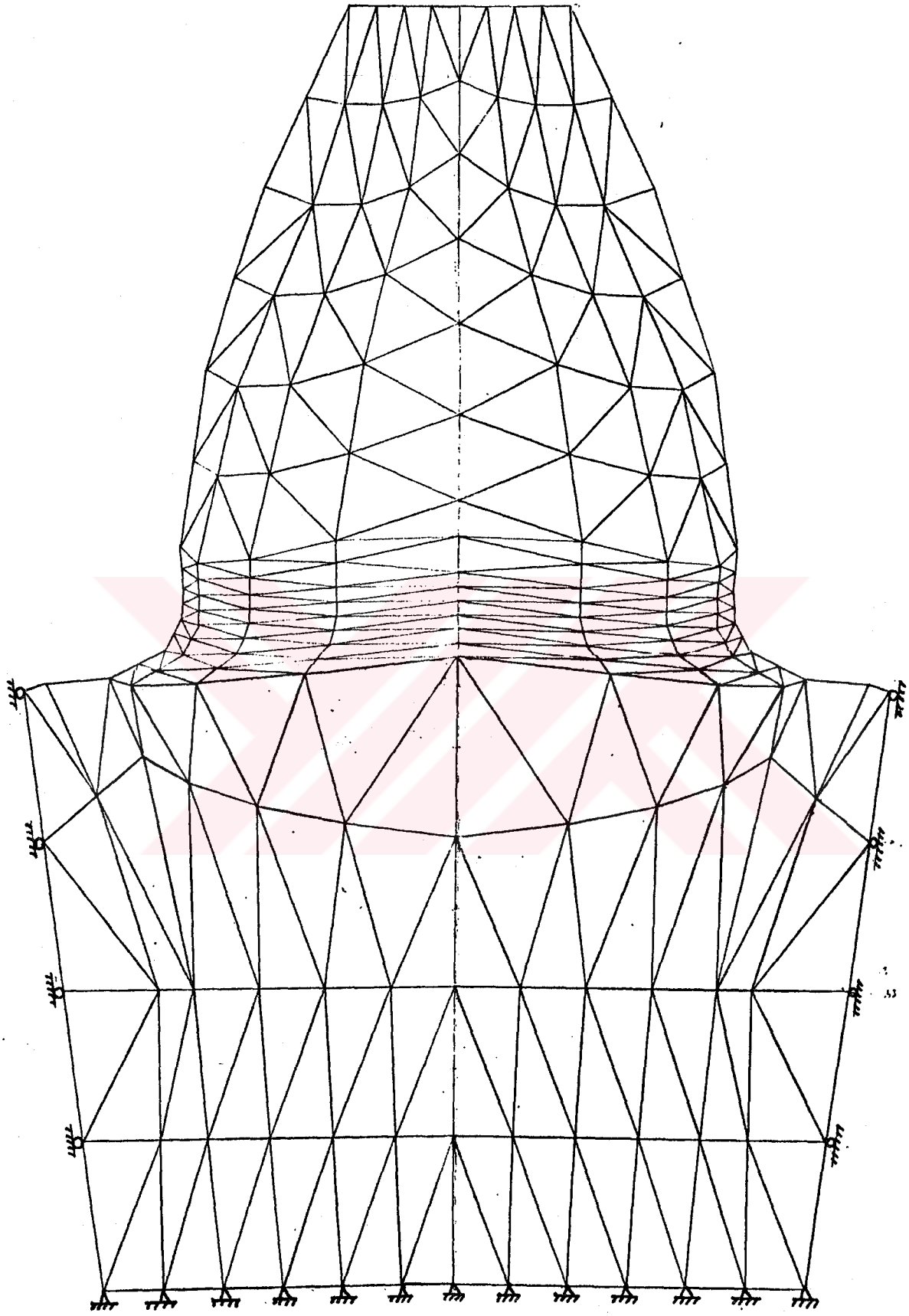

Figure 5.8. FEM model of spur gear tooth used in this study.

The model that is used in this study is given in Figure 5.8. The model have 320 elements with 191 nodes. The model is supported along the base, and guided on both sides. This is very near to the actual physical shape.

5.2.2. Definition of Boundary Conditions

All boundary conditions except force point are given in a data file. So, the program takes it automatically. Because of the physical structure of the spur gear tooth, fixed and guided nodes are related only the sizes of gears. Then all boundaries are fixed to these parameters.

In spur gear stress analysis, definition of force point is very important. In this program, the force point can be defined at the tip or any other node. The highest point of single tooth contact can also be determined. For this purpose user must choose the highest point of single tooth contact as a forcing point. Then the subroutine CONT runs and determines this point for all spur gears.

5.2.3. Generation of Involute Profile

Generation of an involute gear tooth profile is given theoretically in section 3.2. In this work, a computer subprogram INVOL is prepared by using the formulas that were explained in section 3.2. This subroutine generates an involute spur gear tooth with all details automatically. Input of this subroutine are ; module, number of teeth, addendum, dedendum, fillet radius and pressure angle that are the general specifications of any gear. The only constraint is the difference between dedendum circle and base circle must be greater than the fillet radius. The accuracy of the profile that is depending on the number of points on it, is examined by many trials.

5.2.4. Automatic Mesh Generation

Incorrect element data is a major source of errors when running

any finite element program. The preparation of the element data is also a time consuming task. Programs that are automatically generate the element data are available. These programs operate on different principles, but all perform the same mission ; they locate the node points within a region and than subdivide the region into elements. The final result is output of the element node numbers and coordinate information.

In this program a general purpose subroutine GRID is used. GRID uses a group of eight node (quadratic) quadrilateral regions to define the body under consideration. This program is capable of modeling two dimensional domains that are composed of rectangles and triangles having second-order curved boundaries. The element nodes are numbered, and the bandwidth quantity is calculated within the program.

5.2.5. Assembly and Solution of Equations

The key factor in any finite element program is the subroutine for the solution of simultaneous equations. The choice of technique depends upon the size of problem and upon the type of computer available.

In the simplest formulation of the equations are completely formed. This approach requires storage equal to N^2 ,where N is the number of equations, and is possible only where the problem size is small and the computer storage is large.

Two methods of solution have been highly developed for the solution of the simultaneous equations ;

a) *Direct Solution,* in which an exact (within round-off) solution is sought

b) *Iteration,* in which a successive approximation technique is used to converge on the true solution.

The *Gauss Elimination Procedure* is used for direct solution, and the *Gauss-Seidel Procedure* for iterative solution.

In this program, Gauss elimination with back substitution is used. In section 4.2.5 it was stated that after the alterations, all force components had numerical values and so a classical solution of ;

$$F = K\,U$$

would give all components of U. Gauss elimination technique can be used at this stage. Let a set of N equations can be represented in partitioned form as ;

$$\begin{bmatrix} K_{11} & K_{12} \\ K_{21} & K_{22} \end{bmatrix} \begin{bmatrix} \delta \\ \delta \end{bmatrix} = \begin{bmatrix} F_1 \\ F_2 \end{bmatrix}$$

where K_{11} is a 1X1 matrix
K_{12} is a 1X(N-1) matrix
K_{21} is a (N-1)X1 matrix
K_{22} is a (N-1)X(N-1) matrix

δ is a vector of unknowns and F a vector of known values. Then the Gaussian elimination procedure allows the reduction of the K matrix to on N-1 matrix equation of the form ;

$$K^* U = F^*$$

where $K^* = K_{22} - K_{21} K_{11}^{-1} K_{12}$

$$F^* = F_2 - K_{21} K_{11}^{-1} F_1$$

This procedure may be repeated by partitioning K in the same way. The fundamental operation is the triple product $K_{21}\ K_{11}^{-1}\ K_{12}$.

Since K_{11} is (1X1), the number of operations is proportional to

(N-1)². When the matrix K is reduced to a 1X1 matrix, direct solution is possible for the last unknown δ_n .

Back substitution may now be applied to solve for the remaining δ's from equation of the type :

$$\delta_1 = K_{11}^{-1} F_1 - K_{11}^{-1} K_{12} \delta_2$$

This product represents the simplest direct method in which all terms of the matrix are stored and operated upon. However, it is possible to take advantage of the symmetry that exists in structural stiffness matrices by restricting operations to the upper diagonal area, whereupon the number of operations is reduced approximately by half. The total number of operations for solution is about ($N^3/6$).

The typical assemled matrix contains many zero terms, and in particular there is a distance from the diagonal beyond which no term exist. This is called banding of the matrix and the distance from the diagonal term to the last term in any row is called the semi-bandwidth. The banded nature ofthe matrix may be demonstrated by partitioning the matrix as shown below, where a zero submatrix replaces that part of K which has zero values i.e. :

$$K = \begin{bmatrix} K_{11} & K_{12} & 0 \\ K_{12}^T & K_{22} & K_{23} \\ 0 & K_{23}^T & K_{33} \end{bmatrix}$$

Symmetry has been assumed and the matrix sizes are as follows ;

K_{11} is (1X1)
K_{12} is (1XM)
K_{22} is (MXM)
K_{23} is (MX(N-1-M))
K_{33} is ((N-1-M)X(N-1-M))

When K is eliminated only K is modified as the zero submatrix causes no change in K and K . The number of operations in an elimination is now proportional to M^2 and total number of operations to

$$\left[\frac{1}{2}\sum_{n=1}^{N} M_n^2\right]$$

or approximately to

$$\left[\frac{1}{2} N M_{max}^2\right]$$

where M_{max} is the maximum semi-bandwidth.

In practice semi-bandwidth is usually less than 10% of the matrix size, and the band-matrix technique as described reduces the arithmetic to some 3 % of that without taking advantage of banding.

A further advantage is the compaction of storage that can result since the matrix can be stored in a rectangular NXM_{max} array as is shown in Figure 5.8. However, the total number of equations that can be solved will be limited by the size of the rectangular array.

$$\left[\begin{array}{c|c|c|c|c} K_{11} & K_{12} & & & \\ \hline K_{12}^T & K_{22} & K_{23} & K_{24} & \\ \hline & K_{23}^T & K_{33} & K_{34} & \\ \hline & K_{24}^T & K_{34}^T & K_{44} & K_{45} \\ \hline & & & K_{45}^T & K_{55} \end{array}\right]$$

Figure 5.9.a. Original square matrix

$$\left[\begin{array}{c|c|c} K_{11} & K_{12} & 0 \\ \hline K_{22} & K_{23} & K_{24} \\ \hline K_{33} & K_{34} & 0 \\ \hline K_{44} & K_{45} & 0 \\ \hline K_{55} & 0 & 0 \end{array}\right]$$

Figure 5.9.b. Rectangular representation

To reduce computer storage requirements, the large equation solver of the program uses a one dimensional vector to store the upper triangular part of the stiffness matrix that is currently needed at the time of elimination of the uppermost equation. The column-wise storage order was choosen because it is easier to implement than the row-wise order.

5.3. RESULTS

By using the developed package, different variations of spur gears are examined. For this purpose, several runs are made and 24 of them are presented in this thesis. The results of these runs demonstrate the effects of gear parameters on the stresses and the validity of previous works.

The output of the finite element program lists the two axial stresses in x- and y-directions, shear stress,principal stresses and maximum shear stress with the centroidal coordinates for a mesh element. In this section, stress distributions along the tooth profile and on the weakest section of the tooth, effects of gear parameters on results and comparison of the results with previous works are discussed.

5.3.1. Stress Distribution

In Figures 5.10 and 5.11 are shown the stress distribution on a tooth surface acted on by a concentrated unit load located at the tip of the tooth and on the pitch circle level, respectively.

The internal stress distribution on the weakest section of the gear tooth for different loading conditions, modules, and pressure angles are shown in Figures 5.12 to 5.19.

5.3.2. Effects of Gear Parameters on Gear Stresses

In Figure 5.20, changing of stresses with respect to different mating gears are given. This shows a curve that the stresses are decreasing with increasing the mating gear teeth number.

In Figures 5.21 and 5.22 show the changing of stresses with respect to the tooth fillet radius. This is also a curve and the relation can be formulated as follows ;

$$\frac{\sigma_1}{\sigma_2} = \left(\frac{RF_2}{RF_1}\right)^{0.40}$$

Figure 5.23 shows the changing of stresses with respect to forcing point from tip to pitch level.

5.3.3. Comparison of Results with Previous Works

The obtained tooth stresses for the cases mentioned above are given in Table 5.1. Because the stress-strain relationship within an element is assumed to be constant, the exact location of a stress value within an element is unknown. Due to this, the value of stresses at the fillet of the tooth must be found by averaging the neighbouring elements. The stresses obtained by this method and some of the previous works are presented in Table 5.2.

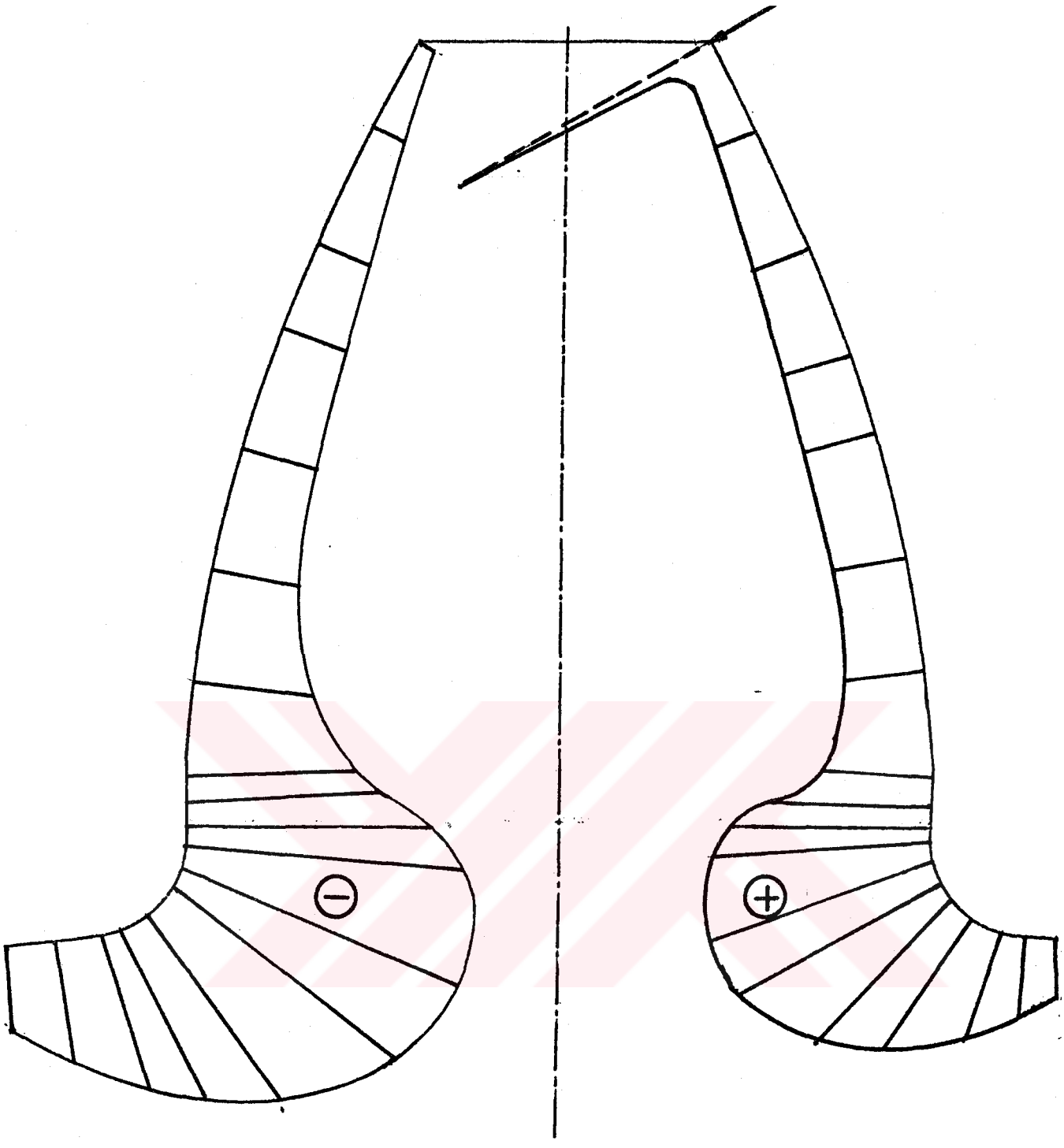

Figure 5.10. The stress distribution on a tooth surface for tip loading condition (results obtained for 18 teeth pinion,20 degree pressure angle 25 mm module, 7.5 mm fillet radius and standard dedendum to addendum ratio is 1.25).

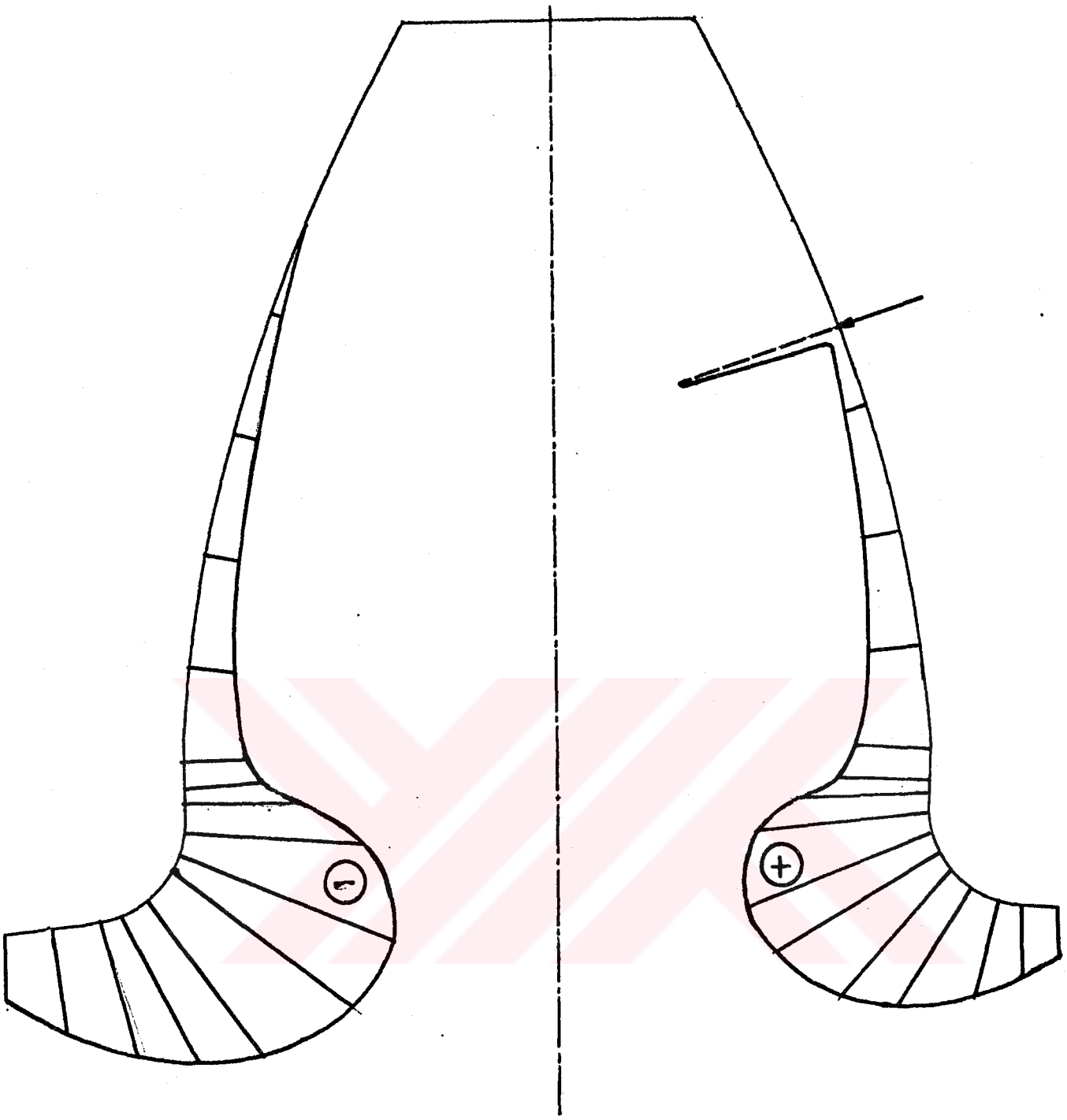

Figure 5.11. The stress distribution on a tooth surface when the load is applied from pitch circle level (results obtained for 18 teeth pinion,20 degree pressure angle, 25 mm module, 7.5 mm fillet radius and standard dedendum to addendum ratio is 1.25).

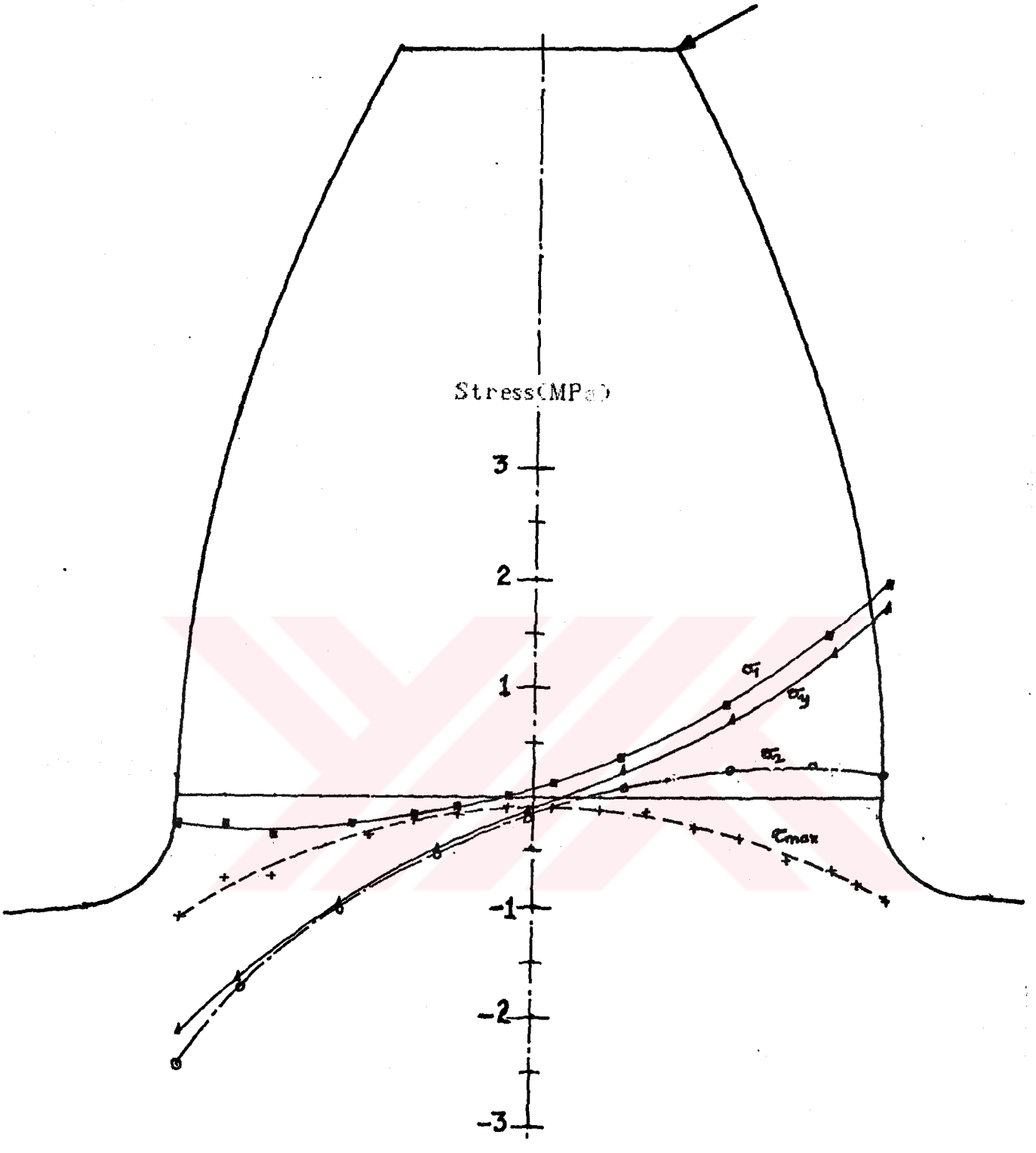

Figure 5.12. The stress distribution along the weakest section on a tooth for tip loading condition (results obtained for 18 teeth pinion,20 degree pressure angle, 25 mm module, 7.5 mm fillet radius and standard dedendum to addendum ratio is 1.25).

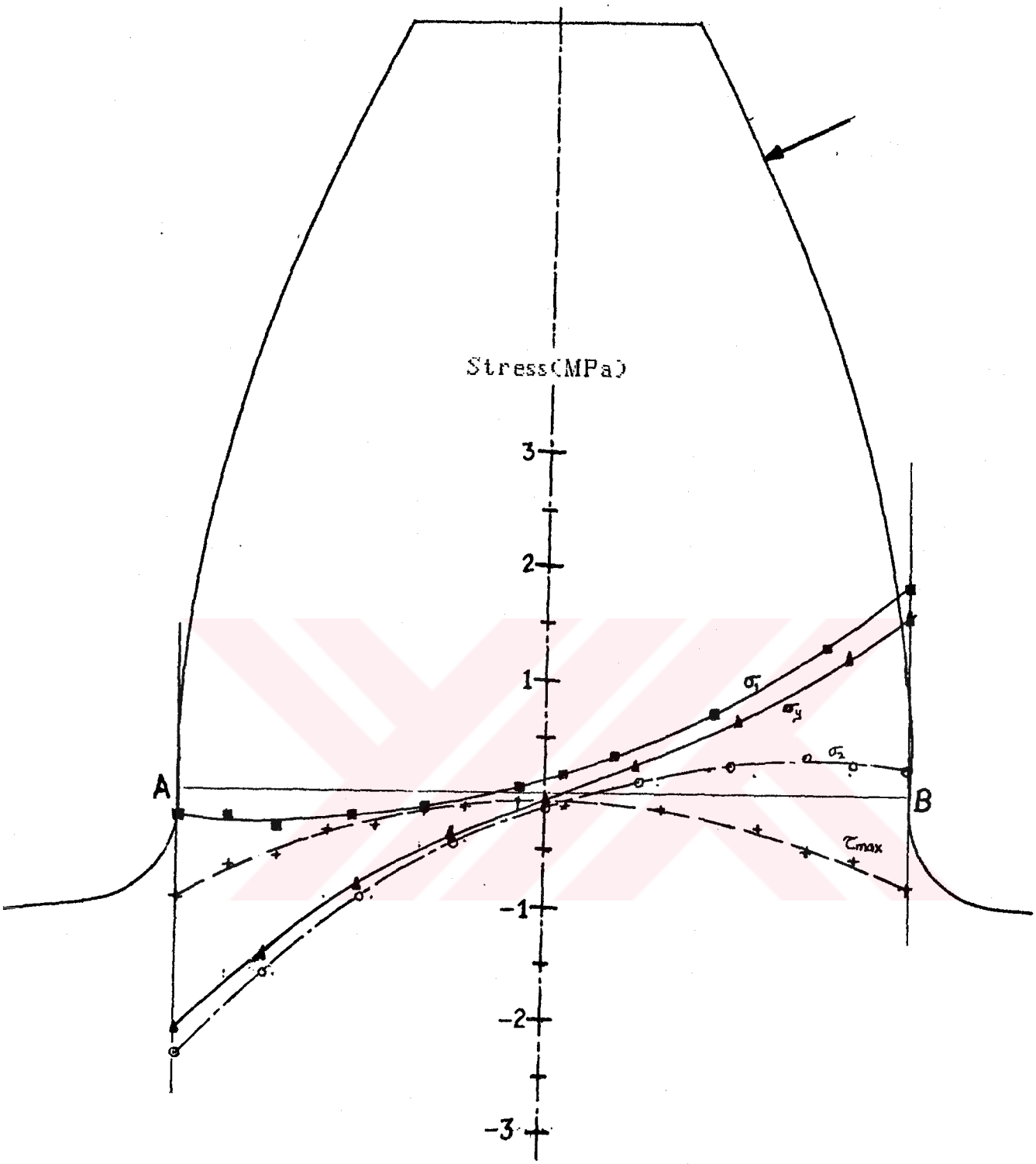

Figure 5.13. The stress distribution along the weakest section on a tooth for the load below the tip of the tooth (results obtained for 18 teeth pinion,20 degree pressure angle, 25 mm module, 7.5 mm fillet radius and standard dedendum to addendum ratio is 1.25).

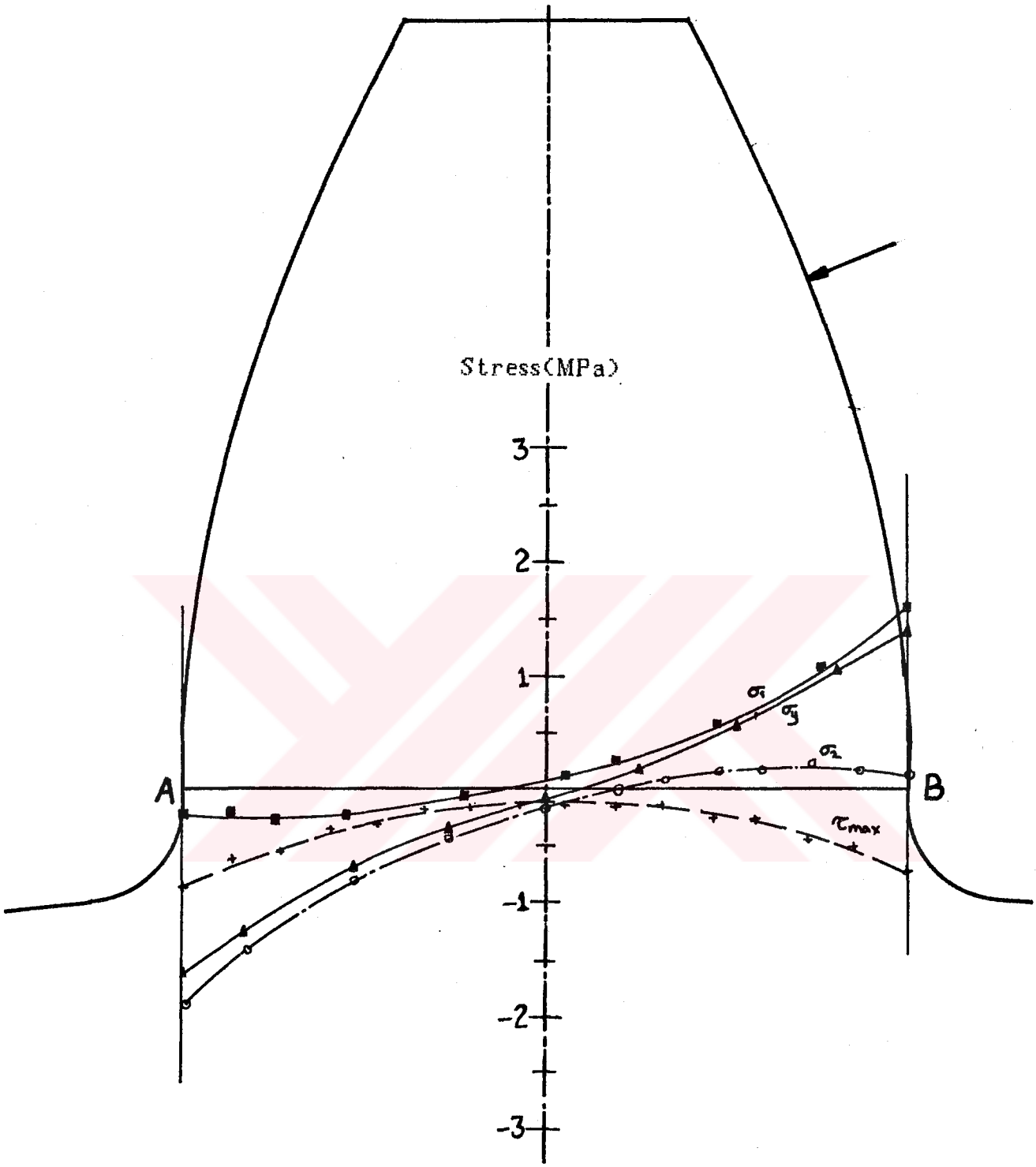

Figure 5.14. The stress distribution along the weakest section on a tooth for the load above the pitch circle level (results obtained for 18 teeth pinion,20 degree pressure angle, 25 mm module, 7.5 mm fillet radius and standard dedendum to addendum ratio is 1.25).

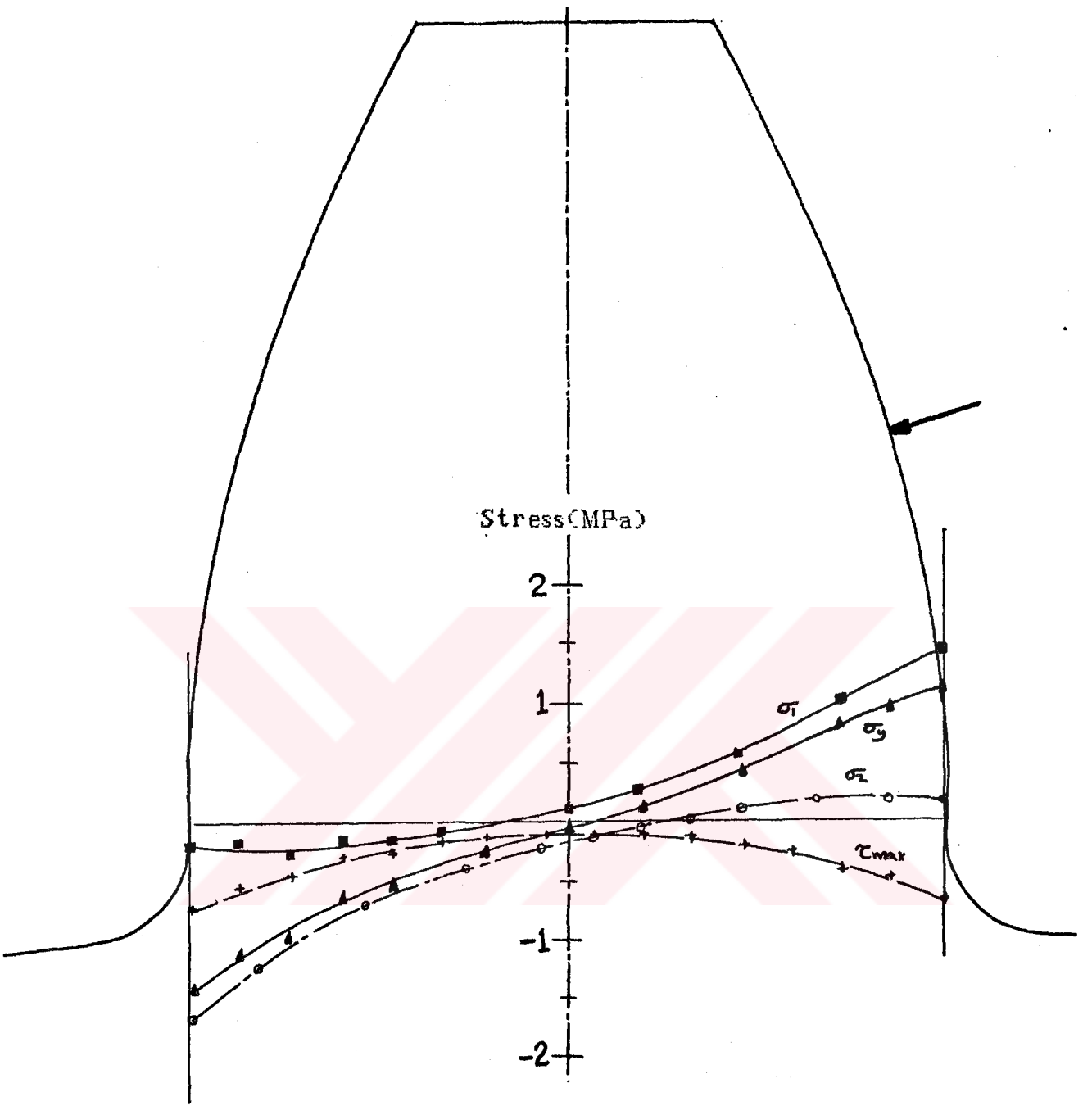

Figure 5.15. The stress distribution along the weakest section on a tooth for the load applied at the pitch circle level (results obtained for 18 teeth pinion,20 degree pressure angle, 25 mm module, 7.5 mm fillet radius and standard dedendum to addendum ratio is 1.25).

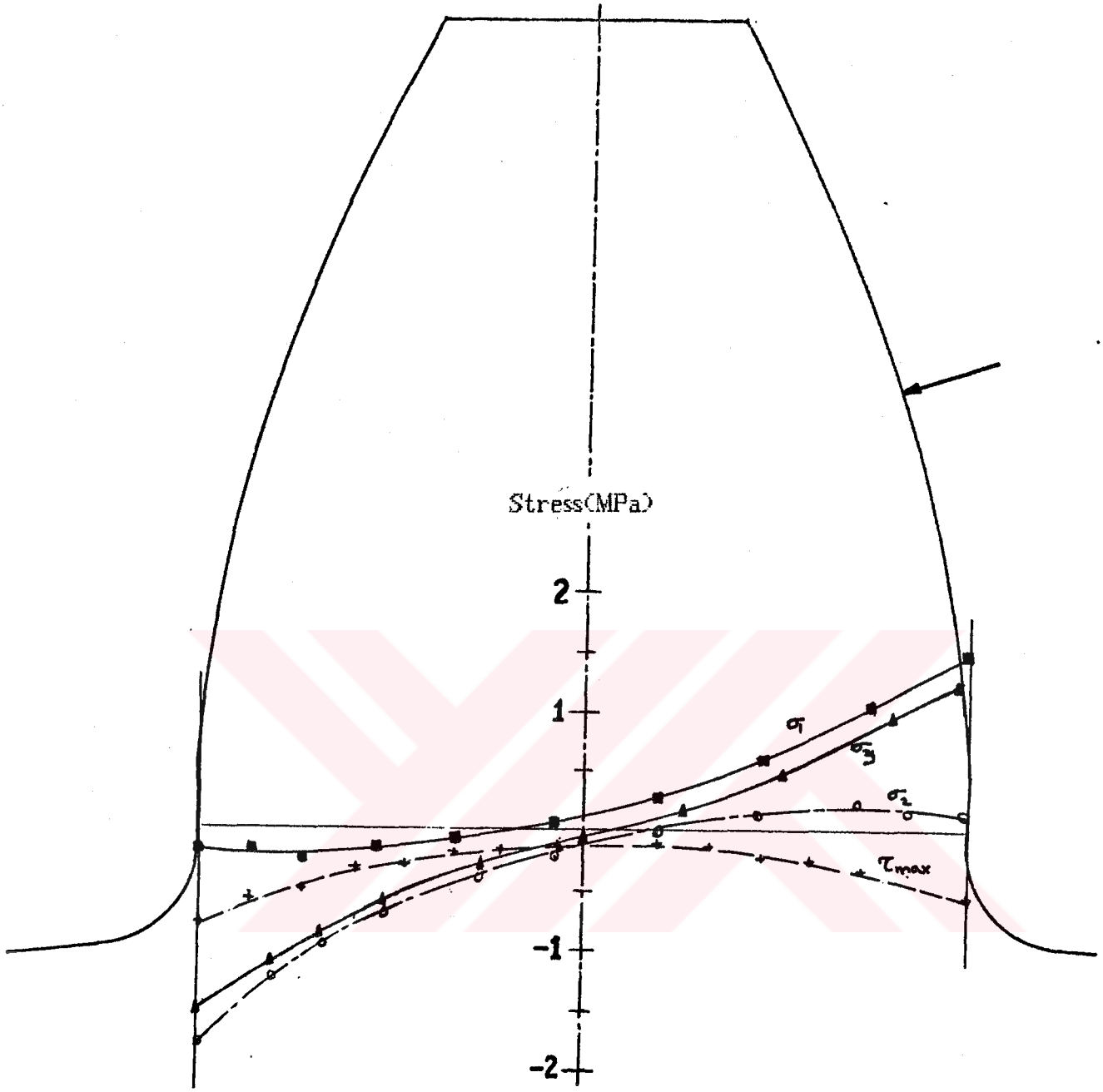

Figure 5.16. The stress distribution along the weakest section on a tooth for the load applied at the highest point of single tooth contact (results obtained for 18 teeth pinion,20 degree pressure angle, 25 mm module, 7.5 mm fillet radius and standard dedendum to addendum ratio is 1.25).

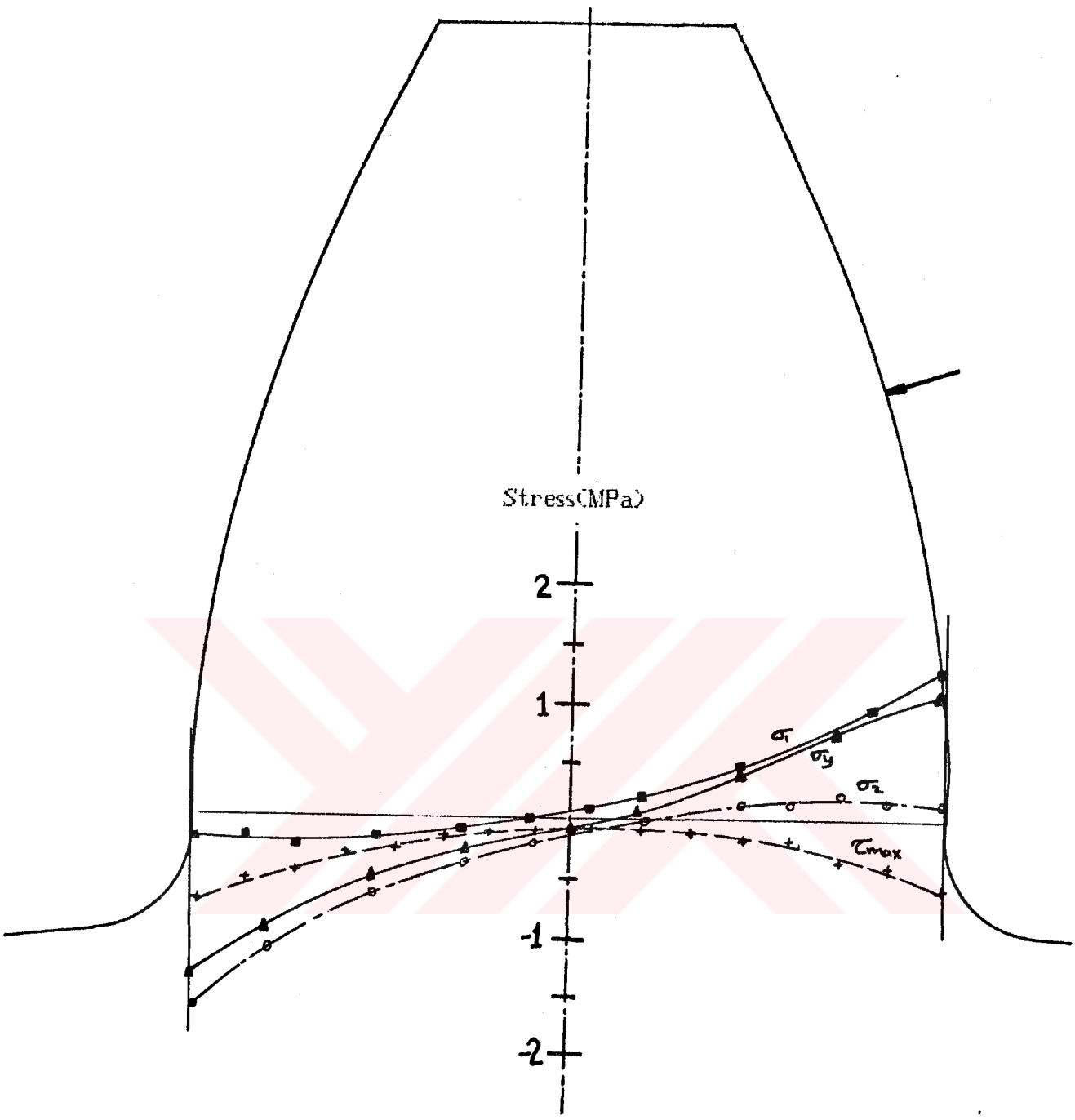

Figure 5.17. The stress distribution along the weakest section on a tooth for the load applied at the highest point of single tooth contact (results obtained for 18 teeth pinion,25 degree pressure angle, 25 mm module, 7.5 mm fillet radius and standard dedendum to addendum ratio is 1.25).

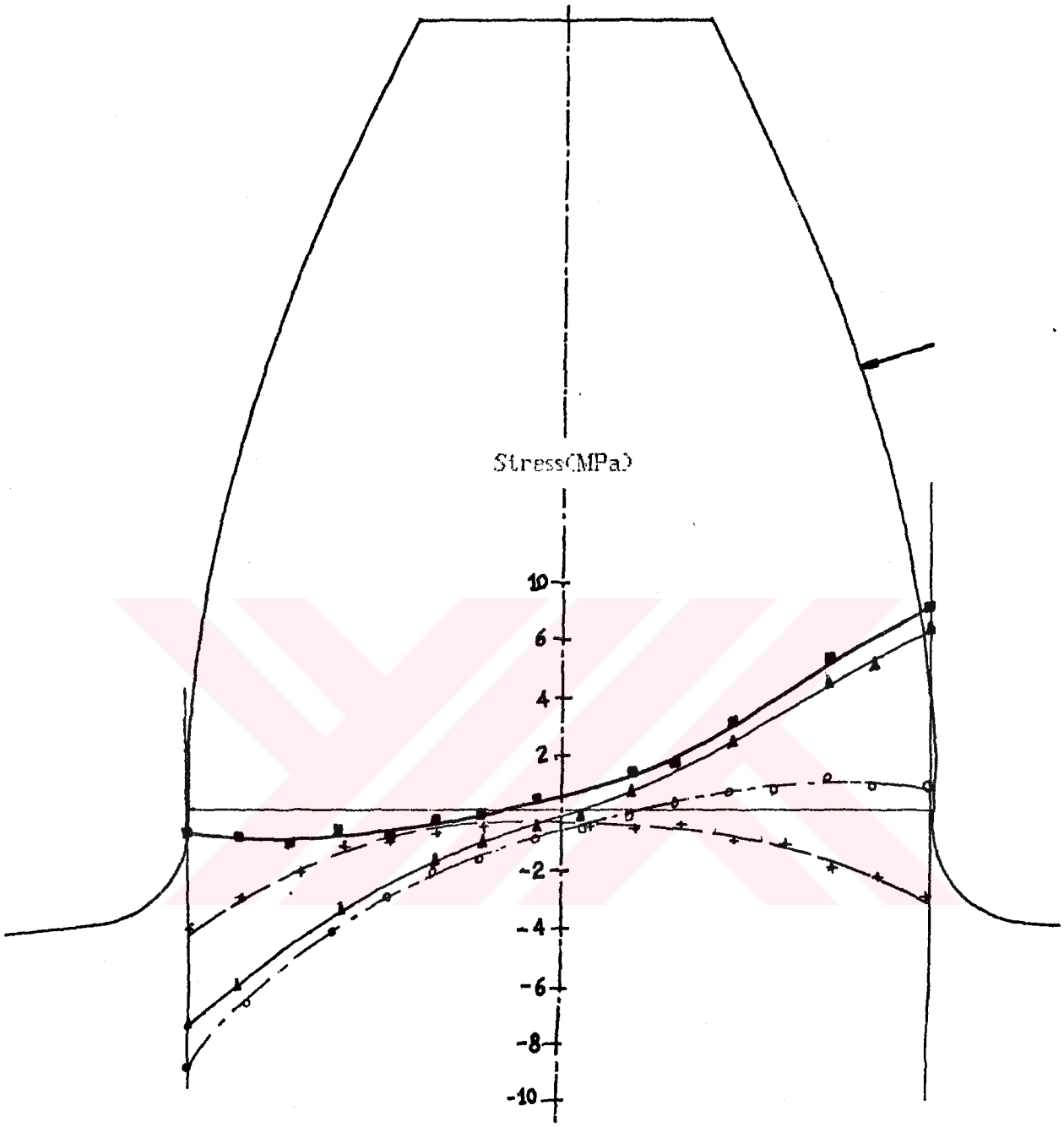

Figure 5.18. The stress distribution along the weakest section on a tooth for the load applied at the highest point of single tooth contact (results obtained for 18 teeth pinion,20 degree pressure angle 5 mm module, 1.5 mm fillet radius and standard dedendum to addendum ratio is 1.25).

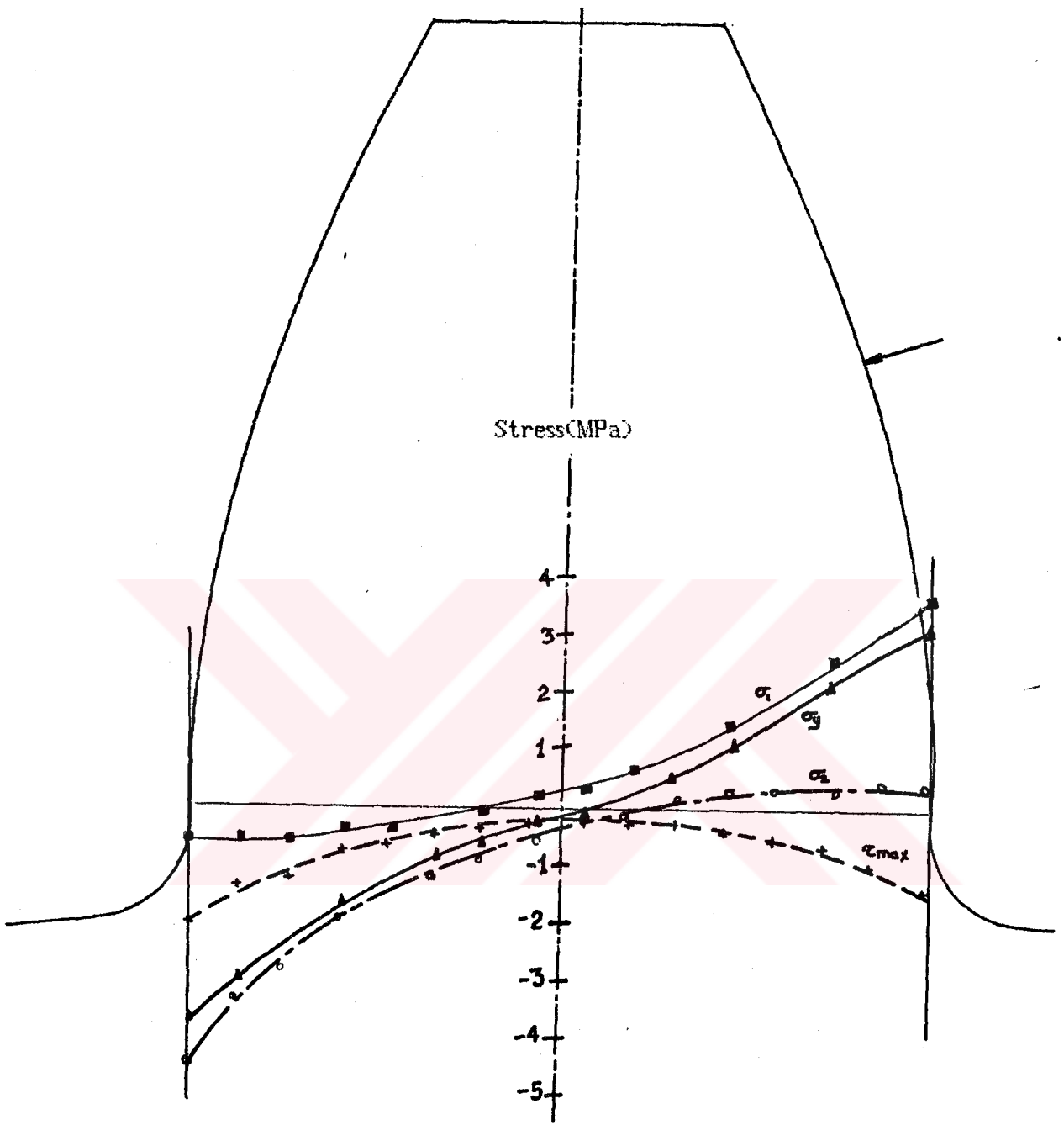

Figure 5.19. The stress distribution along the weakest section on a tooth for the load applied at the highest point of single tooth contact (results obtained for 18 teeth pinion,20 degree pressure angle 10 mm module, 3.0 mm fillet radius and standard dedendum to addendum ratio is 1.25).

Gear specifications

Module = 25 mm
# teeth on pinion=18
# teeth on gear=50
Pressure Angle = 20 degree
Fillet Radius = 7.5 mm

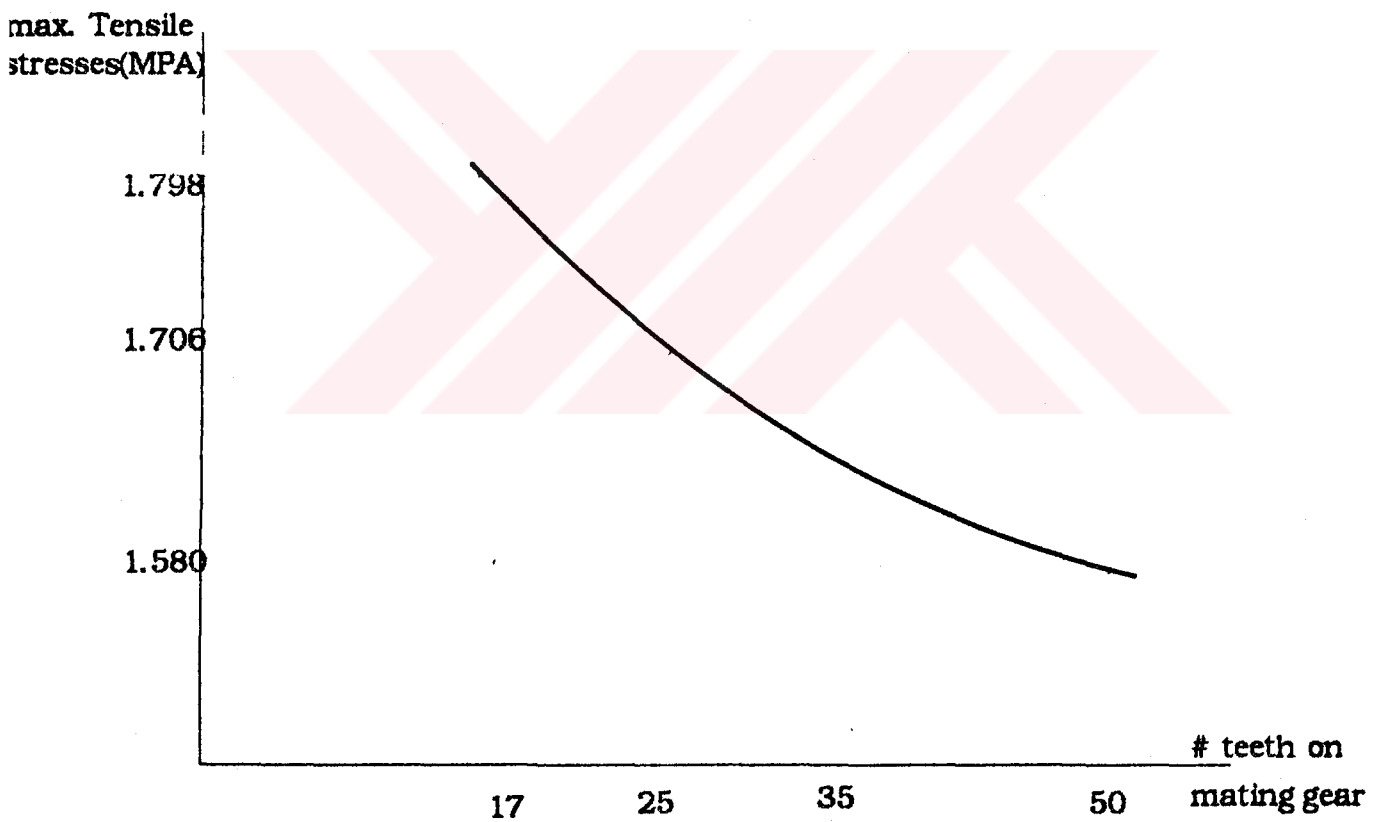

Figure 5.20. Changing of stresses with the # of mating gear

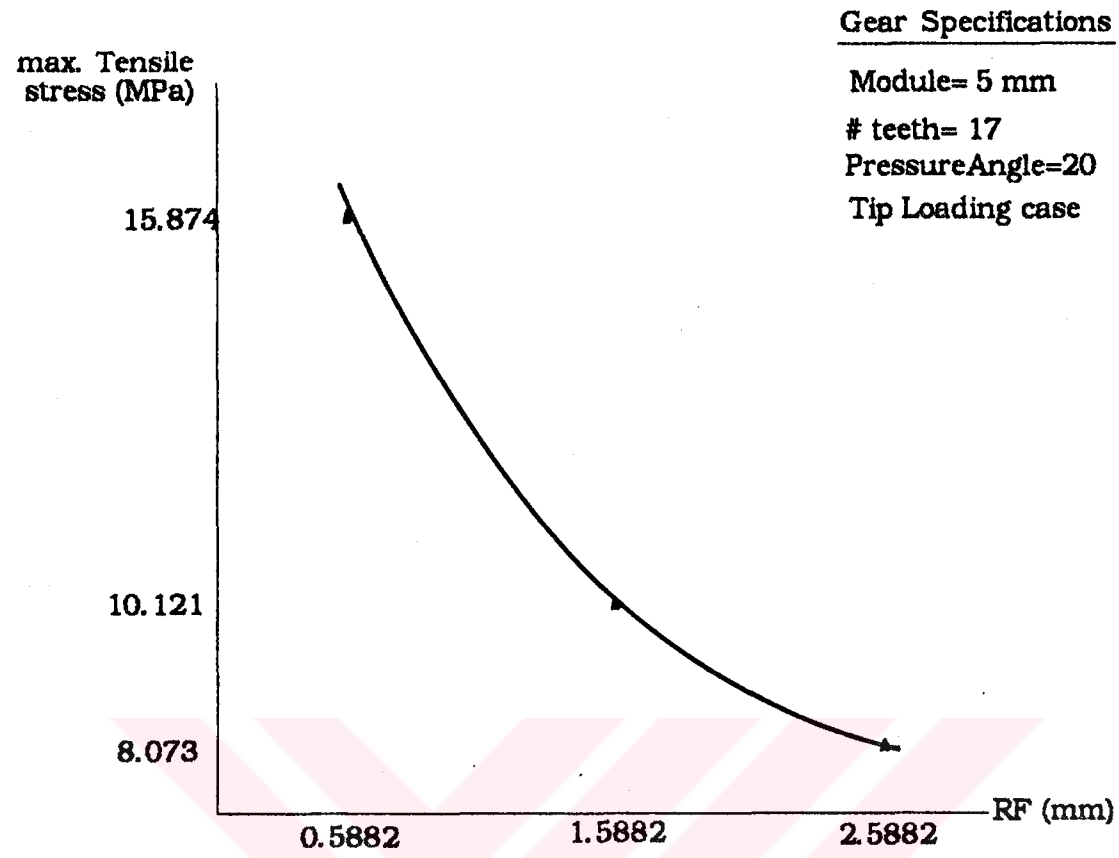

Figure 5.21. Changing stresses with Fillet Radius

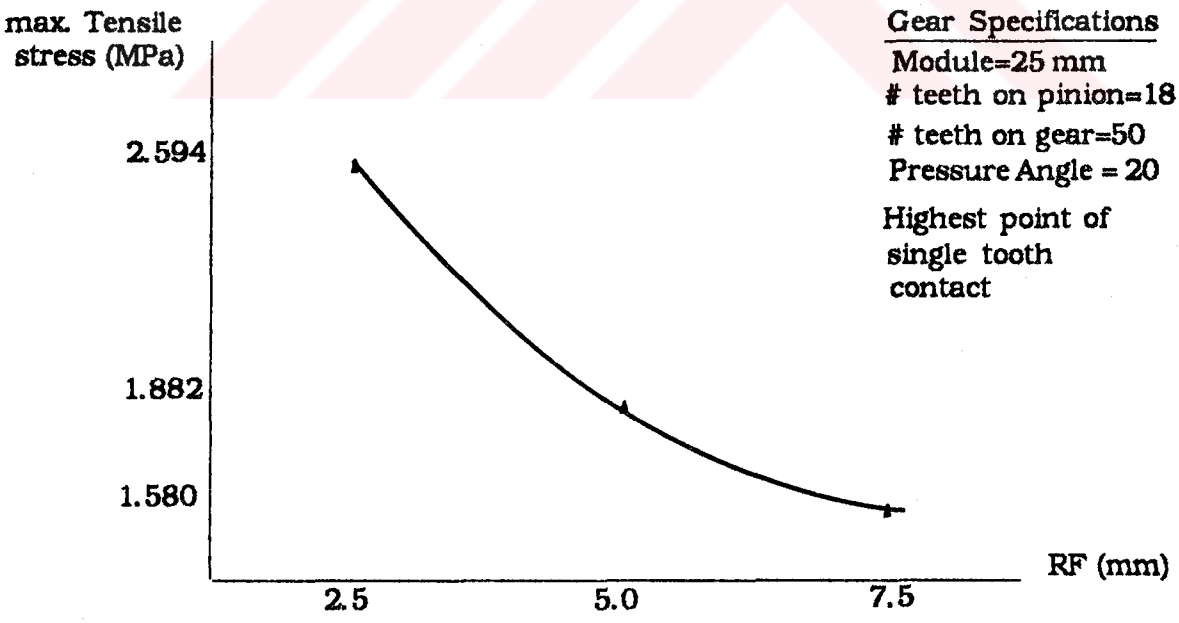

Figure 5.22. Changing stresses with Fillet Radius

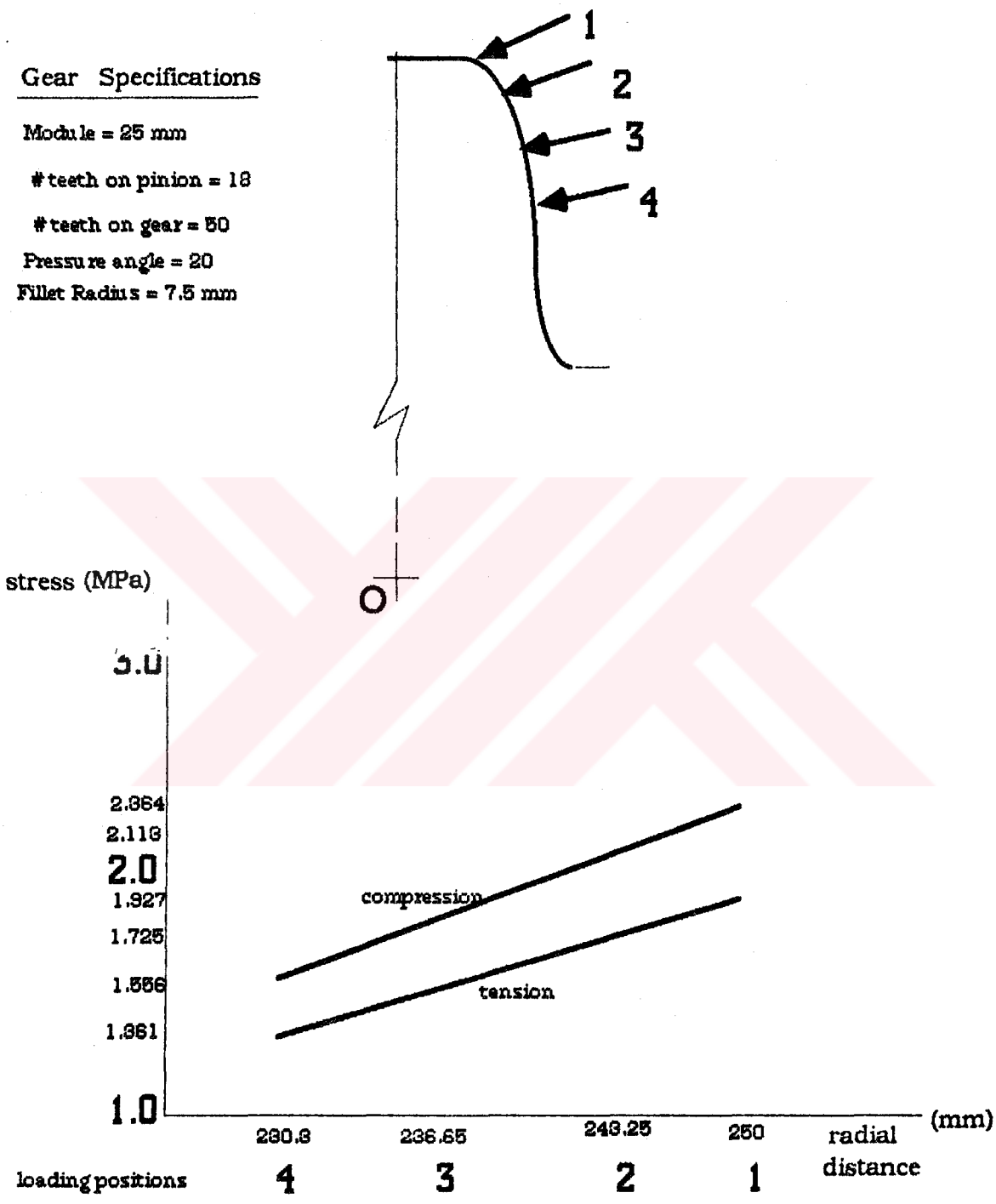

Figure 4.23. Stress variation with respect to forcing point

NP	NG	M	∅	RF	load	Principal stresses				von mises		max shear	
						Comp		tension		C	T	C	T
13	-	5	20	2.769	T	10.21	0.726	8.555	0.893	9.870	8.148	4.743	3.831
13	-	5	20	0.5882	T	22.22	3.866	17.08	3.722	20.67	15.56	9.178	3.831
17	-	5	20	0.5882	T	18.79	3.552	15.87	3.557	17.29	14.42	7.622	6.159
17	-	5	20	1.5882	T	12.36	1.327	10.12	1.501	13.08	9.460	5.521	4.31
17	-	5	20	2.5882	T	9.603	1.093	8.073	0.901	9.108	7.662	4.[illegible]	[illegible]
30	-	25	20	2.5882	T	2.06	0.247	1.714	0.289	1.948	1.589	0.906	0.713
17	20	5	20	2.5882	S	8.172	0.934	7.00	0.788	7.747	6.646	3.618	3.108
17	30	5	20	2.5882	S	7.699	0.871	6.652	0.745	7.303	6.312	3.414	2.953
17	40	5	20	2.5882	S	7.407	0.831	6.445	0.720	7.028	6.116	3.287	2.862
17	50	5	20	2.5882	S	7.207	0.804	6.308	0.704	6.84	5.987	3.201	2.802
18	25	25	20	7.5	S	2.03	0.288	1.706	0.266	1.9024	1.589	0.871	0.720
18	50	25	20	7.5	S	1.855	0.261	1.580	0.245	1.739	1.472	0.797	0.667
18	50	25	20	7.5	T	2.494	0.285	2.036	0.239	2.364	1.921	1.105	0.898
18	50	25	20	7.5	T2	2.229	0.254	1.822	0.214	2.113	1.724	0.987	0.804
18	50	25	20	7.5	T3	1.982	0.280	1.670	0.260	1.857	1.556	0.851	0.705
18	50	25	20	7.5	T4	1.699	0.192	1.468	0.168	1.611	1.361	0.754	0.635
18	50	25	25	7.5	S	1.685	0.252	1.362	0.236	1.547	1.260	0.717	0.563

TABLE 5.1

continue to **TABLE 5.1**

NP	NG	M	∅	RF	load	Principal stresses				von mises		max shear	
						Comp		tension		C	T	C	T
18	50	25	20	5.0	S	2.192	0.361	1.882	0.362	2.035	1.729	0.915	0.76
18	50	25	20	2.5	S	2.882	0.599	2.594	0.592	2.634	2.354	1.141	1.00
18	50	10	20	3.0	S	4.638	0.653	3.949	0.613	4.348	3.680	1.993	1.668
18	50	5	20	1.5	S	9.275	1.305	7.898	1.226	8.696	7.362	3.985	3.336
18	17	25	20	7.5	S	2.155	0.245	1.798	0.281	2.043	1.6752	0.955	0.759
20	25	25	20	7.5	S	1.947	0.280	1.628	0.258	1.823	1.515	0.834	0.685
30	25	25	20	7.5	S	1.673	0.25	1.383	0.235	1.563	1.281	0.712	0.574

T-tip loading

T-T2-T3-T4-tip to pitch level

S- load at the highest point of single tooth contact

THE VALUE OF LOAD THAT IS USED IN CALCULATIONS IS 10 N

NP	NG	M	ø	RF	load	FESA		CHABERT		AGMA	TOBE
						comp. average	tension average	compr	tension	tension	tension
13	-	5	20	2.7692	T	8.5710	6.700	10.230	8.769	-	-
13	-	5	20	0.5882	T	14.911	10.592	13.307	11.846	-	-
17	-	5	20	0.5882	T	12.520	10.136	11.823	10.470	-	-
17	-	5	20	1.5882	T	9.642	7.800	10.647	9.294	-	-
17	-	5	20	2.5882	T	7.948	6.210	9.470	8.1176	-	-
30	-	25	20	7.5	T	1.560	1.2797	1.791	1.5511	-	1.471
17	20	5	20	2.5882	S	6.334	5.40	6.25	5.50	-	5.865
17	30	5	20	2.5882	S	5.972	5.133	6.00	5.40	-	5.260
17	40	5	20	2.5882	S	5.846	4.975	5.95	5.25	-	4.914
17	50	5	20	2.5882	S	5.598	4.873	5.85	5.20	-	4.692
18	25	25	20	7.5	S	1.553	1.234	1.338	1.168	0.893	1.070
18	50	25	20	7.5	S	1.378	1.123	1.279	1.117	1.092	0.907
18	50	25	20	7.5	T	1.918	1.553	2.101	1.834	-	1.633
18	50	25	25	7.5	S	1.240	0.966	1.435	1.253	0.868	1.1112
18	50	25	20	5.0	S	1.589	1.387	1.347	1.184	-	-
18	50	25	20	2.5	S	1.861	1.508	1.415	1.252	-	-

TABLE 5.2

Continue to **TABLE 5.2**

NP	NG	M	ø	RF	load	FESA		CHABERT		AGMA	TOBE
						comp. average	tension average	compr	tension	tension	tension
18	50	10	20	3.0	S	3.445	2.858	3.1992	2.793	2.7313	2.268
18	50	5	20	1.5	S	6.890	5.704	6.398	5.586	-	4.535
18	17	25	20	7.5	S	1.660	1.301	1.380	1.205	1.159	1.196
20	25	25	20	7.5	S	1.440	1.173	1.275	1.111	1.0899	1.0211
30	25	25	20	7.5	S	1.220	0.979	1.0975	0.950	0.9742	0.9151

CHAPTER 6

DISCUSSION AND CONCLUSION

6.1. INTRODUCTION

The efficiency and capability of the prepared computer program and gear tooth stresses are discussed in section 6.2. Conclusion of the study is given in section 6.3. In section 6.4 suggestions to future work is given.

6.2. DISCUSSION

6.2.1. Computer Program

In the previous chapters, the evaluation of spur gear tooth stresses are studied. The Finite Element Method is used as a tool. For this purpose a finite element stress analysis program is developed.

For structural analysing, a number of very large capacity programs have been developed. But they are general purpose programs, and the cost of the packages are very high. Determination of a gear tooth stresses is a very special topic. So that, by using a general purpose finite element structural analysis program, the determination of tooth profile is very difficult. A highly skilled user is necessary with the enough knowledge on the involumetry of a gear tooth. Also the number of input for working with such a program is so much.

All the conditions that are necessary for generation of spur gear and rack profiles, are inserted into the developed program. The only

input of the program are ; module, number of teeth of gears (for a rack, only the number of teeth of pinion), pressure angle and tooth fillet radius that are the general specifications of any gear.

All boundary conditions except force point is determined by the program itself. For determination of the value of force and the forcing point is dependent on the user's choice. When program begins to run, it gives three choices to user for determination of forcing point. These are ;

i) force is acting on the tip of the tooth
ii) force is acting at the highest point of single tooth contact
iii) any other point that will be determined by user.

The program has the capability of analysing the tooth stresses of spur gears and racks for all the conditions explained above. The highest point of single tooth contact is calculated automatically by the program taking the contact ratio into account.

The only constraint of the program for a spur gear is that the difference between the radius of base circle and the radius of the dedendum circle is greater than the tooth fillet radius. For this condition and for undercut, the program gives an error massage to the user changing these conditions for any run.

For minimizing the computation time, and computer storage requirements, the bandwidth technique is used in the evaluation of the stiffness matrix and in the solution of equations.

The output of the program is an organized form and very easy to understand. So that, the program can be used easily by anyone who knows a little about the gears.

6.2.2. Gear Tooth Stresses

In this study, many different cases of spur gears are examined by using the developed program. The results for 24 runs show that the

changing of tooth stresses with respect to the changing of forcing point from tip of the tooth to the pitch circle level, is linear. But the slope of this line is not equal to the contact ratio. This linearity demonstrates the validity of Henriot's approach. In Henriot's approach ; for a given pinion, the stress resulting from a load applied at the highest point of single tooth contact is in a constant ratio to the stress resulting from the same load divided by the contact ratio and applied at the tip of the tooth. This is not a good method in the analysing of tooth stresses because of the difficulty of determination of the constant ratio that is necessary for obtaining exact values of the stresses.

The relation between tooth fillet stresses and fillet radius are examined and a formula between them is obtained. Fillet radius is highly effective on the tooth stresses ; the small decrease in radius causes rapid increase in fillet stresses.

The module and force are directly related with the stresses.Force is directly proportional and the module is inversely proportional to the stresses.

Increase in number of teeth of mating gear decreases the stresses. The relation is a polynomial function similar to the formula between tooth fillet radius and the stresses.

The formula given by T.Tobe,M.Kato, and K. Inoue [58] is valid only to a specific condition that they have used. Their formula not contains the effect of pressure angle, fillet radius,number of teeth of mating gear and contact ratio. Also, the location of the highest point of single tooth contact should be calculated before using their formula.

The formula suggested by L.Wilcox and W.Coleman [66] is not practical. It requires many calculations for determinations of paramaters in the formula. So that, a computer subprogram is necessary for using this formula.

The formula given by Chabert [57] contains many of the gear parameters. It seems to be applicable for all standard gears (20 degree pressure angle, standard dedendum and addendum ratio is 1.25, and zero addendum modification). But it still needs some modifications.

It can be seen that from Table 5.2, the results obtained by this package have greater values than the results of Chaberts [57] and AGMA gear tooth fillet stress equations. The differences between results are mostly due to the generation of the tooth profile below the base circle that is not involute.The determination of the location of point S (which is the common point of tangent line between the starting point of involute profile and the fillet circle) is a difficult problem. In this study, the location of this point is carefully inspected and exact location is determined.

The other important factor that affects the results is the forcing point. The worst loading condition for a gear tooth is the highest point of single tooth contact. The determination of this point is another important step of this study. A practical formula is given for the determination of this point.

6.3. CONCLUSION

In this study, the tooth stresses of spur gears and racks are evaluated by using Finite Element Method. A computer aided stress evaluation package has been prepared. This package is very efficient in evaluation of the tooth fillet stresses of spur gears and racks. The finite element models of spur gear and rack are prepared also.

With this program 24 runs are made and effects of gear parameters on tooth stresses are examined. The stress distributions along the tooth profile and inside the tooth for different conditions are obtained. The results are compared with the previous works.

The developed program can be used in the design of other machine elements by some modifications. Also, this study may lead to new studies in different areas of mechanical engineering that will use the Finite Element Method.

6.4. SUGGESTIONS FOR FUTURE WORK

Evaluation of gear tooth stresses can be extended to the following cases ;

1) The generation of tooth profile for the case of (RB-RD) < RF and undercutting.

2) An addendum modification can be considered.

3) Same work can be done for other external and internal types of gears.

4) The stiffness can be calculated.

LIST OF REFERENCES

1) Lewis, W. "Investigation of Strength of Gear Teeth ", Proceedings Engineering Club, Philedelphia 10(1892) No.1, p.16-23.

2) DIN 3990, "Load Capacity Computation of Spur and Bevel Gears", Dec.1970.

3) AGMA Standard 220.02, "Strength of Spur Gear Teeth',1966.

4) Dolan, Broghamer, " A Photoelastic Study of Stresses in Gear Tooth Fillets",Eng. Exp. State Univ. of Illionis, Bulletin 3/35 31+9.

5) Niemann, G., Machine Elements, vol. II, Springer, Berlin, 1960.

6) Niemann, G., "Dedendum Strength of Steel Spur Gears", VDI-Zeitchrift, 1950, p. 923.

7) Heywood, "Tensile Fillet Stresses in Loaded Projections",Proc. Inst. Mech. Eng. 159 ,1948.

8) Kelley and Pedersen, "Dedendum Strength in Modern Gear Construction", Antriebstechnik, vol.18, Vieweg, Braunschweig, 1957.

9) Mitchiner, R.G., and Mabie, H.H., "The Determination of Lewis Form Factor Y and AGMA Geometry Factor J for External Spur Gear Tooth ", Virginia Polytechnic Inst. and State Univ.

10) Shigley, J.E.,"Mechanical Engineering Design ", 4'th ed., Mc Graw Hill, Kagakuska, 1983.

11) Yelle, H., "A Microcomputer Program to Calculate Spur Gears", Ecole Polytechnique de Montreal Raymond Gauvin.

12) The AGMA Standard 226.01, Information Sheet, "Geometry Factor for Determining the Spur Gear Teeth".

13) N.K. Al-Id, "A Theoretical Method for the Determination of the Stress Concentration Factors of Gear Teeth", Proc. of the 1989 Int. Power Transmission and Gearing Conference.

14) R. W. Clough, "The Finite Element Method in Plane Stress Analysis" Proceedings of 2nd ASCE Conference on Electronic Computation, Pittsburgh, Pa., September 7, 1960.

15) R. Courant,"Variational Methods for the Solutions of Problems of Equilibrium and Vibrations", Bull. Ame. Math. Soc. vol. 49, 1943.

16) L. Euler, Methods Invenienndi Lineas Curvas Maximi Minimine Proprietate Gaudentes, M. Bousquet, Lausanne and Geneva, 1974.

17) G. Polya, "Sur une Interpretation de la Methode des Difference Finies qui peut Fournir des Bornes Superieeures ou Inferieures," C. R. Acad. Sci., Vol 235, 1952.

18) G. Polya, Estimates for Eigevalues: Studies Presented to Richard von Mises, Academic Press, New York, 1954.

19) J. Hersch. "Equations Differentielles et Functions de Cullules," C. R. Acad. Sci., Vol. 240, 1955.

20) H. F. Weinberger, "Upper and Lower Bounds for Eigenvalues by Finite Difference Methods," Commun. Pure Appl. Math., Vol. 9, 1956.

21) H. F. Weinberger, "Lower Bounds for Higher Eigenvalues by Difference Methods," Commun. Pacific J. Math., Vol. 8, 1958.

22) J. Greenstadt, "On the Reduction of Continuous Problems to Discrete Form," IBM J. Res. Dev., Vol. 3, 1959.

23) P. M. Morse and H. Feshback, Methods of Theoretical Physics, McGraw-Hill Book Company, New York, 1953, Section 9.4.

24) G. N. White, "Difference Equations for plane Thermal Elasticity," LAMS-2745, Los Alamos Scientific Laboratory, Los Alamos, N. Mex., 1962

25) K. O. Frederichs, "A Finite Difference Scheme for the Neumann and the Dirichlet Problem," NYO-9760, Courant Institute of Mathematical Scieces, New York Universty, New York, 1962.

26) J. T. Oden Finite Elements of Non-linear Continua, McGraw-Hill Book Company, New York, 1972.

27) G. Birkhoff and H. L. Garabedian, "Smooth surface Interpolation," J. Math. Phys., Vol. 39, 1960.

28) C. de Boor, "Bicubix Spline Interpolation," J. Math. Phys., Vol. 41, 1962.

29) G. Birkhoff and C. de Boor , "Piece-wise Polynomial Interpolation and Approximation," in Approximation of Functions, H. L. Garabedian (ed.), Elsevier Publishing Company, Amsterdam, 1965.

30) J. H. Ahlberg, E. N. Nilson, and J. L. Walsh, The Theory of Splines and Their Applications, Academic Press, New York, 1967.

31) W. J. Gordon and D. H. Thomas, "Cardinal Functios for Splines Interpolation," General Motors Res. Rept. GMR-770, 1968.

32) W. j. Gordon, "Distributive Lattices and the Aproximation of Multivariate Functions," Proceedings of the Sympoosium on Approximation ith Spetial Emphasis on Spline Functions, held at the Mathematics Research Center, University of Wisconsin, May 5-7, 1969, Academic Press, New York, 1969.

33) I. J. Schoenberg (ed.), Approximations with Special Emphasis on Spline Funtions, Academic Press, New York, 1969.

34) W. J. Gordon, "Spline-Blended Surface Intepolation Though Curve Networks," J. math. Mech. Vol. 18, no. 10, 1969.

35) T. N. E. Greville (ed.), Theory and Applications of Sline Functions, Academic Press, New York, 1969.

36) R. s. Varga, "Functional Analysis and Aproximation Theory in Numerical Analysis," SIAM (Regular Conference Series in Applied mathematics), Philadelphia, Pa., 1971.

37) W. G. Strang and G. Fix, An Analysis of the Finite Element Method, Prentice-Hall, 1973.

38) I. Babuska and A. K. Aziz (des.), The Mathematical Foundations of the Finite Element Method-with Applications to Partial Differential Equations, Academic Press, New York, 1973.

39) J. Whiteman (ed.), the Mathematics of Finite Elements and Applications, Academic Press, New York, 1973.

40) J. F. Besseling, "The Complete Analogy Between the Matrix Equations and the Continuous Field Equations of Structural Analysis," International Symposium on Analogue and Digital techniques App;ied To Aeronautics, Liege, Belgium, 1963.

41) R. J. Melosh, "Basis for the Derivation of Matrices for the Direct Stiffness Method," AIAAJ., Vol. 1, 1963.

42) B. Fraeijs de Veubeke, "Upper and Lower Bounds in Matrix Structural Analysis," in Agard-ograph 72, B. F. de Veubeke (ed.), Pergamon Press, New York, 1964.

43) R. E. Jones, "A Generalization of the Direct-Stiffness Method of Structural Analysis," AIAAJ., Vol. 2, 1964.

44) O. C. Zienkiewicz and Y. K. Cheung, 'Finite Elements in the Solution of Field Problems," Engineer, Vol. 220, 1965

45) S. W. Key, "A Convergence Study of the Direct Stiffness Method," Ph. D. Dissertation, Universiyt of Washington, Seattle, Wash., 1966.

46) R. W. McLay,"Completeness and Convergence Properties of Finite Element Displacement Function-A Genaral treatment,"AIAA 5th Aerospac Science Meeting(AIAA Paper 67-143),New york,1967.

47) P. Tong and T. H. H. Pain, "The convergence of the Finite Element Method in Solving Linear Elastic Problems," Int. J. Solids Struct., Vol. 3, 1967.

48) E. R. de Arentes e Oliveria, "Completeness and Convegance in the Finite Element Method," Procedings of the 2nd Conference on Matrix methods in Structural Mechanics (AFFDL-tr-68-150), Wright-Patterson Air force base, Dayton, Ohio, October 1968.

49) M. W. Johnson and R. W. McLay, "Convergence of the Finite Element in the Theory of Elasticity," J. Appl. Mech., Vol. 35, No. 2, June 1968.

50) J. E. Waltz, R. E. Fulton, N. J. Cyrus, "Accurasy and Convergence of Finite Element Approximations," Proceedings of the 2nd conferece on Matrix Methods in Structural Mechanics (AFFDL-TR-68-150), Wright-Patterson Air Force Base , Dayton, Ohio, October 1968.

51) P. C. Dunne, "Complete Polynominal Displacement Fields For the Finite Element Method," J. Roy. Aeronaut. Soc., 72, 1968.

52) H. Ramstad, "Convergence and Numerical Accuracy with Spetial Reference to Plate Bending,"in Finite Element Methods in Stress Analysis, I. Holand and K. Bell (eds.), Tapir Press, Trondheim, Norway, 1969.

53) A. Zenisek and M. Zlamal , "Convergence of a Finite Element Procedure for Solving Boundary Value Problems of the Fourth Order," Int. J. Numer. Methods Eng., Vol. 2, 1970.

54) M. Mikkola, "On the Convergence of the Finite Element Method," 4th Scandinavian Meeting on Strength of Materials, Helsinki, 1971.

55) E. R. de Arentes e Oliveira, "Convergence Thoerems in the Theory of Structures," in the NATO Lectures on Finite Element Methods in Continuum Mechanics, J. T. Oden and E. R. A. Oliveira (eds.), University of Alabama Press, Huntsville, Ala., 1972.

56) Zeinkiewics,O.C.,"The Finite Element Method in Engineering Science",2nd edition, New York, Mc.Graw-Hill, 1971.

57) Chabert, G.,Tran, T.D.,and Mathis, R.,"An Evaluation of Stresses and Deflection of Spur Gear Teeth Under Strain", Journal of Eng. and Industry, February 1974.

58) Tobe, T.,Kato, M.,Inoue, K., "True Stress and Stiffness of Spur Gear Tooth",Proceedings of 5th World Congress on Theory of Machines and Mechanisms, 1979,published by ASME.

59) Drago, R.J., Pizzigati, G.A.,"Some Progress in the Accurate Evaluation of Tooth Root and Fillet Stresses in Light Weight, Thin Rimmed Gears", AGMA paper 229.21,Fall technical Meeting, Washington DC, October 1980.

60) Castellani, G., Castelli, V.P.,"Rating Gear Strength", Transactions of ASME, vol.103, April 1981.

61) Hwang, J.E., Dennis, A.G., and Weichel, J.F., "Computer Aided Design of the Stress Analysis of an Internal Spur Gear", Gear Technology, May/June 1988.

62) Eiff, H.V., Hirschmann, K.H., and Lechner, G., "Influence of Gear Tooth Geometry of EXternal and Internal Gear", Proc. of the 1989 Int. Power Transmission and Gearing Conference.

63) Ustinenko, V.L.,"Influence of some Parameters on the Bending Stress in Spur Gear Teeth",Transactions for Machine Design, No.11, 1962, p.33.

64) Aida, T., and Terauchi, Y.,"On the Bending Stress of a Spur Gear", Bulletin of Japanese Society of Mechanical Engineers, vol.5, No.17, 1962,p.161-170.

65) Bağcı, Cemil,"Finite Stress Elements and Application in Machine Design", presented at the 6th Applied Mechanisims Conference, Denver, 1979.

66) Wallace, D.B., and Seireg, A.,"Computer Simulation of Dynamic Stress, Deformation, and Fracture of Gear Teeth", Transactions of ASME, Journal of Eng. for Industry, p.1103, November 1973.